Implementing a new texture-based soil evaporation reduction coefficient in the FAO 2Kc method

Abdelhakim Amazirh, Olivier Merlin, Salah Er-Raki, Elhoussaine Bouras, Abdelghani Chehbouni

Implementing a new texture-based soil evaporation reduction coefficient in the FAO-2Kc method

Abdelhakim Amazirh[a,*], Olivier Merlin[b], Salah Er-Raki[a,c], Elhoussaine Bouras[b,c], Abdelghani Chehbouni[a,b].

[a]*Mohammed VI Polytechnic University (UM6P), Morocco, Center for Remote Sensing Applications (CRSA).*

[b]*Centre d'Etudes Spatiales de la Biosphère (CESBIO), Université de Toulouse, CNES, CNRS, IRD, UPS, Toulouse, France.*

[c]*ProcEDE, Département de Physique Appliquée, Faculté des Sciences et Techniques, Université Cadi Ayyad, Marrakech, Maroc.*

Corresponding author*: Dr. Amazirh Abdelhakim

Email: **abdelhakim.amazirh@um6p.ma/** abdelhakim.amazirh@gmail.com

Center for Remote Sensing Applications (CRSA), Mohammed VI Polytechnic University (UM6P), Hay Moulay Rachid-Benguerir, Morocco.

Abstract

Crop evapotranspiration (ET) is a fundamental component of the hydrological cycle, especially in arid/semi-arid regions. The FAO-56 offers an operational method for deriving ET from the reduction (dual crop coefficient K_c) of the atmospheric evaporative demand (ET_0). The dual coefficient approach (FAO-2Kc) is intended to improve the daily estimation of ET by separating the contribution of bare soil evaporation (E) and crop transpiration components. The FAO-2Kc has been a well-known reference for the operational monitoring of crop water needs. However, its performance for estimating the water use efficiency is limited by uncertainties in the modeled evaporation/transpiration partitioning. This paper aims at improving the soil module of the FAO-2Kc by modifying the E reduction coefficient (K_r) according to soil texture information and state-of-the-art formulations, hence, to amend the mismatch between FAO-2Kc and field-measured data beyond standard conditions. In practice this work evaluates the performance of two evaporation models, using the classical Kr ($K_{r,FAO}$) and a new texture-based Kr ($K_{r,text}$) over 33 bare soil sites under different evaporative demand and soil conditions. An offline validation is investigated by forcing both models with

observed soil moisture (θ_s) data as input. The $K_{r,text}$ methodology provides more accurate E estimations compared to the $K_{r,FAO}$ method and systematically reduces biases. Using $K_{r,text}$ allows reaching the lowest root means square error (RMSE) of 0.16 mm/day compared to the $K_{r,FAO}$ where the lowest RMSE reached is 0.88 mm/day. As a step further in the assessment of the proposed methodology, ET was estimated in three wheat fields across the entire agricultural season. Both approaches were thus inter-compared in terms of ET estimates forced by SM estimated as a residual of the water balance model (online validation). Compared to ET measurements, the new formulation provided more accurate results. The RMSE was 0.66 mm/day (0.71 mm/day) and the R^2 was 0.83 (0.78) for the texture-based (classical) Kr.

Keywords: FAO-2Kc, soil evaporation, soil texture, soil moisture, evapotranspiration.

1. Introduction

Surface evapotranspiration (ET) is an important flux in water and energy exchange processes at the interface between land surfaces and the atmosphere. Soil evaporation (E) is one of the main components of ET beside plant transpiration. E accounts for a substantial part of ET from the exposed soil surface in growing crops, where its spatial distribution plays an important role in various fields such as hydrology, meteorology and agronomy. In addition, E is the only hydrological flow that connects both water (through soil moisture) and energy (through land surface temperature) balances. About 50 % to 70 % of annual precipitation is consumed by E to the atmosphere which is considered as a water loss and not used for crop productivity (Harrold et al., 1959; Peters, 1960; Wallace, 2000).

Partitioning ET is essential in modeling land atmosphere interactions and vegetation water uptake and it is crucial in the monitoring of plant water uptake and water stress (Er-raki et al., 2010; Merlin et al., 2016; Porporato et al., 2001; Rafi et al., 2019). In agricultural crops, water is mainly lost by E during the germination and emergence stage of growing crops. Then, through the crop growth and development, the surface is covered; therefore, E impacts less the water change in the soil while the transpiration becomes the main process and dominates ET. In arid and semi-arid regions including irrigated areas, E is the main outward flux and influences the soil water budget, which is very vital for agriculture (Suleiman and Ritchie, 2003). Schlesinger and Jasechko, (2014) reported that the E contribution into ET ranges from 20 % to 40 %, and it is an essential boundary condition between soil and atmosphere.

It is well known that the E process occurs in two main stages. The first stage is characterized by a constant rate of E which is also known as the energy-limited stage. It corresponds to when the evaporation occurs at a maximum rate meaning that it is limited only by the external meteorological (radiation, wind speed and relative humidity) conditions. This stage continues as long as the soil underneath has enough water storage. The second stage, also named the falling rate stage, corresponds to when the surface dries so that the evaporation becomes limited by soil moisture (θ_s) and by the soil hydraulic properties that determine the transfer of liquid and vaporized water to the surface. In this stage the soil resistance to water diffusion increases until θ_s reaches its minimal value (Chanzy et al., 1993). The rate of evaporation and the duration of both stages vary with soil texture. Therefore, more water can be evaporated from saturated clayey soil than from saturated sandy soils because more water is stored in a clayey soil than in a sandy soil.

Different techniques have been used to measure E. Among them, we cite weighing lysimetry (Balwinder-Singh et al., 2011; Boast and Robertson, 1982; Leuning et al., 1994), isotopy (Aouade et al., 2016; Zhang et al., 2011) and portable evaporation chamber (Luo et al., 2018; Raz-Yaseef et al., 2010). Recently, Rafi et al. (2019) intercompared different methods based on eddy covariance, sap flow and weighing lysimetry measurements to assess E. The above techniques provided E measurements at a crop field scale.

The FAO dual crop coefficient model (FAO-2Kc, Allen, 2000) is one of the most widely used models to estimate crop ET due to its simplicity and operationality, and it has been applied in standard and beyond standard conditions (Suleiman et al., 2007). The FAO-2Kc consists in splitting the crop coefficient K_c into two separate coefficients, one for crop transpiration, called the basal crop coefficient (K_{cb}) and one for soil evaporation (K_e). FAO-2Kc model requires limited input parameters and it has been used to simulate ET of crops like wheat (Drerup et al., 2017; Er-raki et al., 2010; Er-Raki et al., 2007; Jin et al., 2017), olive (Er-raki et al., 2008; Er-Raki et al., 2010), citrus (Rallo et al., 2017), table grapes (Er-Raki et al., 2013), sugar beet (Anderson et al., 2017; Diarra et al., 2017) crops grown under different climates (Ayyoub et al., 2017; Debnath et al., 2015).

Despite the numerous applications of FAO-2Kc, many studies reported that the E component is not well quantified. In some studies, the FAO-2Kc method overestimates E at the start of the season and underestimates it at the end of the season (Mutziger et al., 2005; Parlange et al., 1992; Torres and Calera, 2010). Rafi et al., (2019) and Olivera-Guerra et al., (2018) found an underestimation of E at the start and the end of the wheat growing season. This is

potentially due to the classical K_e or more specifically to the reduction coefficient K_r of FAO-2Kc which is based on an ad hoc relationship with texture via the θ_s at field capacity (Merlin et al., 2016). Moreover, Phillips et al., (2017) stated that most land-surface models used to estimate E cannot differentiate soil texture and this is due to the difficulty to incorporate the soil texture effect on the E rate.

Merlin et al., (2016) showed that the nonlinear relationship between E rate and surface θ_s over bare soils varied systematically with soil texture across several well-instrumented sites. Based on this work, a new K_r formula was proposed based on the soil texture information using a new pedo-transfer function that physically links K_r to texture ($K_{r,text}$). The new pedo-transfer function was developed in Merlin et al. (2016) using a meta-analysis approach and was recently corroborated by a physically-based modelling approach relying on soil hydrodynamical properties to simulate capillary flow (Lehmann et al. 2018). This gives independent insight and additional confidence on the robustness of the proposed pedo-transfer function.

The aim of the study is therefore to assess the usefulness of the pedo-transfer function of Merlin et al. (2016) within the FAO formalism using - for the first time - 36 contrasted sites. First, the new ($K_{r,text}$) and classical ($K_{r,FAO}$) formulations are tested over 33 bare (or approximately bare) soil sites with different soil textures and compared against E measurements. In this case, *in situ* soil moisture data are used as forcing (offline validation), by considering the evaporation module separately from the water budget model, meaning that the soil moisture forcing of Kr is measured. Note that among the 33 bare sites used to evaluate the FAO evaporation estimates in the offline mode, 32 sites belong to the calibration data set of Merlin et al. (2016) while the remaining site (MOBou) is used in this paper for the evaluation. Then, as a complementary assessment of the new evaporation formulation, crop ET was retrieved during the entire agricultural season. In this case, the simulated soil moisture (θ_{FAO}) is used as forcing to $K_{r,FAO}$ and $K_{r,text}$ (online validation) by considering the evaporation module coupled to the water budget model, meaning that the soil moisture forcing of Kr is simulated by the FAO water budget model. Both formulations of soil evaporation were evaluated in terms of total ET estimates over three wheat sites located in Morocco near Marrakech. Note that the 3 wheat sites (B123, EC1, EC2) was used in this paper to validate the online implementation of the soil evaporation reduction coefficient in the FAO model. All the three sites do not belong to the calibration data set of Merlin et al. (2016).

2. Sites and data description

In this study, a significant number of sites (33 bare soil and 3 wheat sites) have been used and divided into two categories depending on the desired objectives: i) the 33 bare soil sites have been used for comparing $K_{r,FAO}$ and $K_{r,text}$ under bare soil conditions only, and ii) the 3 wheat plots have been used to evaluate the new evaporation module when coupled to the crop water budget during the entire growing season including all phenological stages of wheat. A description of all the sites is presented below. More details about all the 32 bare soil sites but MOBou can be found in Merlin et al. (2016).

The studied 33 bare soil sites were differing in climatic conditions and soil textures (Table 1). These sites are situated in 13 countries all over the world among which 8 are located over uncropped lands, containing the natural lands including sand desert (NIHAP), savanna fallow (NISav) and degraded land (NIDeg), native grass (AUStu), grass for silage or hay (USDk1), short grass following fireforest (USFwf), and sparse shrub (USMo1 and USMo7). The remaining 25 sites are located over agricultural fields where an identification of bare soil periods is performed. In this study, ‘‘bare soil’’ period is defined as a time period when the plant transpiration is either negligible or small compared to E. Hence the term ‘‘bare soil’’ includes both actual bare soil conditions, and soils partially covered by mulch, crop residue, or sparse vegetation. The data were collected from several national and international flux station networks, intensive field measurements and extracted during bare or quasi bare soil periods by Merlin et al. (2016). Table 1 indicates the localization of the different 33 bare soil sites, where most sites are located in Europe continent. In Table 1 , the clay and sand fractions are presented. The sand fraction ranges from 0.05-0.92 and clay fraction from 0.02-0.56. Such a wide observation range of sand and clay fraction allows for testing the methodologies over different soils. Additional soil physical properties are also given in Table 1 such as, the volumetric soil moisture at saturation (θ_{SAT}), soil moisture at field capacity (θ_{FC}) and soil moisture at wilting point (θ_{WP}) as well as the readily evaporable water (REW). These parameter values are estimated with pedotransfer functions based on clay and sand fractions (Brisson and Perrier, 1991; Cosby et al., 1984; Noilhan et al., 1996).

Table 1: Study sites and their soil physical properties.

Sites	Sand (%)	Clay (%)	θ_{SAT} (m^3/m^3)	θ_{WP}(m^3/m^3)	θ_{FC}(m^3/m^3)	REW (mm)	Country
AUStu	34.3	14.5	0.4079	0.205	0.335	9.5	Australia
BELon	7.5	20	0.4566	0.205	0.335	9.5	Belgium
CHOe2	9.5	43	0.4940	0.23	0.36	10	Switzerland
DEGeb	9.5	30	0.467	0.205	0.335	9.5	Germany
DEKli	21.5	55.7	0.4798	0.22	0.36	10	Germany

DESeh	16.8	12.2	0.4465	0.205	0.335	9.5	Germany
DKVou	92	2	0.3816	0.045	0.12	4.5	Denmark
ESES2	10.4	47.5	0.4963	0.23	0.36	10	Spain
FRAur	20.6	32.3	0.4570	0.205	0.335	9.5	France
FRAvi	13.2	32.8	0.4691	0.205	0.335	9.5	France
FRGri	9.8	18.9	0.4522	0.205	0.335	9.5	France
FRLam	12	54.3	0.4984	0.22	0.36	10	France
FRRE1	5	40	0.4979	0.205	0.335	9.5	France
FRRE2	5	40	0.4979	0.205	0.335	9.5	France
IECa1	57	17	0.3893	0.11	0.23	8	Ireland
ITBCi	32	46	0.4491	0.22	0.36	10	Italy
ITCas	25	22	0.4274	0.15	0.29	9.5	Italy
MEYaq	36	44	0.4387	0.22	0.36	10	Mexico
MOBou	41	18	0.4373	0.15	0.244	8	Morocco
MOSR1	18.5	47	0.4787	0.22	0.36	10	Morocco
MOSR2	18.5	47	0.4787	0.22	0.36	10	Morocco
NIDeg	77	8	0.3835	0.11	0.23	8	Niger
NIHAP	93	5.7	0.3714	0.045	0.12	4.5	Niger
NIMil	77	8	0.3835	0.11	0.23	8	Niger
NISav	77	8	0.3835	0.11	0.23	8	Niger
USArm	28	43	0.4548	0.22	0.36	10	USA
USDk1	48	9	0.3966	0.12	0.25	9	USA
USFwf	30	13	0.4163	0.15	0.29	9.5	USA
USIb1	10	35	0.4791	0.205	0.335	9.5	USA
USIHO	58	28	0.3886	0.205	0.335	9.5	China
USMo1	66	10	0.3860	0.11	0.23	8	USA
USMo7	80	6	0.3847	0.065	0.15	6	USA
USSGP	26	24	0.4301	0.23	0.36	10	USA

In addition to soil texture, continuous measurements of energy fluxes had been monitored in each site such as net radiation (Rn), soil conduction (G) and sensible and latent heat fluxes (H) and (LE), respectively. Measured LE is corrected using the Bowen ratio (Twine et al., 2000). Note that, in some sites LE is missing. In this case, LE is estimated as the residual of the energy balance equation.

The three wheat crops used for evaluating E estimations by simulating total ET are located close to Marrakech, Morocco (Figure 1). This region is characterized by a semi-arid to arid climate with high reference ET and low precipitation. Agricultural areas are generally covered by winter wheat crops. The three winter wheat fields are comprised of one flood irrigation plot (B123) of 4 ha located in an irrigated agricultural zone (called R3) and two drip-irrigated fields, both being 1.5 ha and situated in Chichaoua region. Both regions are located in the Haouz plain. The area undergoes contrasted atmospheric conditions all over the year with high temperature and low rainfall (less than 250 mm/ year) during summer and low temperature and irregular rainfall from autumn to spring with a high evaporative demand (1600 mm/year). Wheat is the dominating crop (50 %) of the R3 zone, which is known for its heterogeneity and contains different types of land cover (alfalfa, wheat, olive, orange and

horticulture). Numerous studies have been carried out since 2002 on this area (Ait Hssaine et al., 2018; Amazirh et al., 2019, 2018, 2017; Chehbouni et al., 2008; Khabba et al., 2013; Ojha et al., 2019; Olivera-Guerra et al., 2020). The Chichaoua site has been monitored since 2016. Both wheat sites in Chichaoua were sown in November 2016, with the same drip irrigation system. One of the plots (EC1) had been irrigated according to FAO crop water requirements and the other plot (EC2) had undergone stress in controlled conditions. Additional details and information about the study sites can be found in Amazirh et al. (2018), Merlin et al. (2018) and Rafi et al. (2019).

During the investigated agricultural seasons, all the three sites were monitored by an eddy covariance system, equipped with different sensors providing continuous measurements of energy and water fluxes exchanged between soil, vegetation and atmosphere. The installed hygrometer provided continuous measurements of H and LE fluxes. Additional instruments were installed in the tower providing extra measurements such as a Sonic 3D anemometer designed to measure the wind speed over the 3 orthogonal axes. R_n was measured by the net radiometer Kipp and Zonen CNR4.

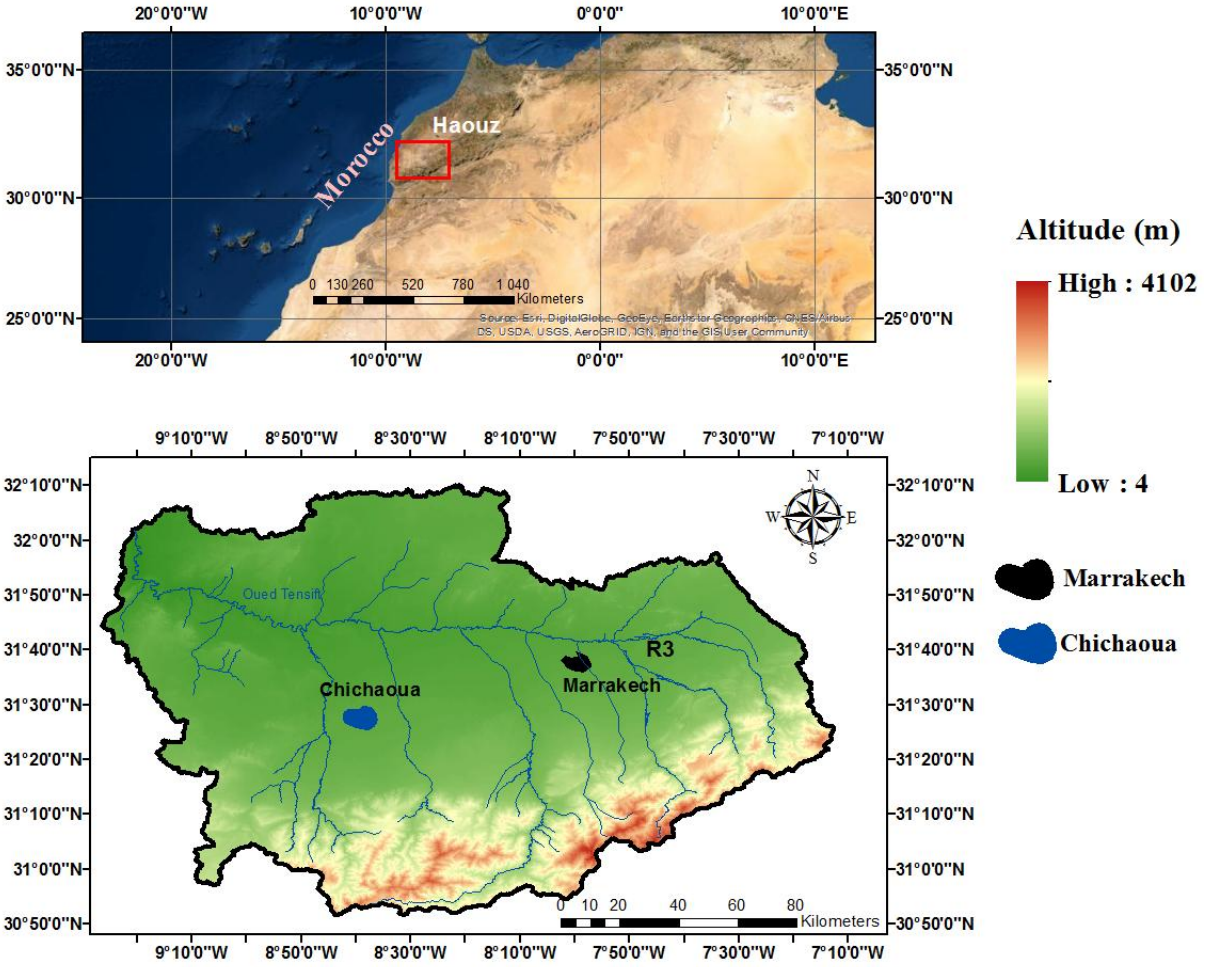

188

189 *Figure 1: Study areas where the coupled approach ($K_{r,text}$-FAO-2Kc) is evaluated.*

190 Half-hourly or sub-hourly measurements of classical meteorological data composed of air
191 temperature T_a, wind speed u_a, incoming solar radiation R_g and air relative humidity rh_a were
192 collected at a reference height (2 m). Soil moisture data were also measured by Time Domain
193 Reflectometry sensors over the 3 sites at different soil depths (5, 10, 15, 30, 100 cm). In this
194 work two surface layers were used: 5 and 10 cm. A mean value between the two layers has
195 been used to assess soil moisture within the 0-10 cm soil column. For the sites where the soil
196 moisture at 10 cm is unavailable and only soil moisture at 5 and 15 cm are available, a
197 linearly interpolation as in Merlin et al. (2011) was used to estimate the integrated soil
198 moisture from 0 to 10 cm depth.

199 # 3. Methodologies

200 ## 3.1. Dual crop coefficient method FAO-56

Allen et al. (1998) describe with details the theoretical background to assess crop ET. The FAO-56 method is based on FAO-24 (Doorembos and Pruitt, 1975), where ET is estimated based on the crop coefficient (K_c) and the reference evapotranspiration (ET_0). Allen, (2000) and Allen et al. (2005b, 2005a, 1998) incorporate the dual crop coefficient, splitting K_c into crop and bare soil contributions. Using the dual crop coefficient method allows for partitioning ET into bare soil evaporation and plant transpiration beyond standard conditions using two coefficients: the soil water evaporation coefficient (K_e) to describe E from the soil surface and the basal crop coefficient (K_{cb}) to describe plant transpiration (Equation 1). The daily variation in the crop coefficient is a function of the wetness of the soil surface and plant development. The crop ET under well-watered conditions is written as (Steduto et al., 2009):

$$ET_c = (K_{cb} + K_e)ET_0 \quad (1)$$

with ET_c being the maximal crop ET, ET_0 being the ET rate over a well-watered crop land covered by a short green, grass-like crop (reference ET), depending only on atmospheric conditions. An adjustment is made to obtain the actual estimates of the real crop ET_a by introducing the water stress coefficient K_s into the Equation (1), and it becomes:

$$ET_a = (K_{cb}K_s + K_e)ET_0 \quad (2)$$

In this paper we aim to improve the representation of E in Equation (2). Under bare soil conditions, crop transpiration is equal to zero (K_{cb}=0). E from Equation (3) is expressed as:

$$E = K_eET_0 \quad (3)$$

Soil evaporative coefficient (K_e) is a function of the amount of water in the soil, soil properties and the exposed and wetted soil fraction to solar radiation where most E occurs (f_{ew}). K_e is defined using Eq. 4:

$$K_e = \min\{[K_r(K_{cmax} - K_{cb})], [f_{ew}K_{cmax}]\} \quad (4)$$

where few = min (1-fc, fw) with fw being the fraction of the soil surface wetted by irrigation or rainfall (fw is 1 in case rainfall) and fc the fraction of surface covered by vegetation, and where K_{cmax} is the maximum value (ranging from 1.05 to 1.30) of crop coefficient K_c following rain or irrigation. It represents the upper limit on E and transpiration that reflects the natural constraints on available energy. For bare soil, K_{cb} is again equal to 0 and K_{cmax} is equal to 1.2 (Allen et al., 2005b, 1998). K_e formula becomes:

$$K_e = K_{cmax} K_{r,FAO} \quad (5)$$

with K_r being the reduction coefficient, which depends on the cumulative depth of water depleted (D_e) and the amount of water that can be depleted by E during a complete drying cycle (TEW). Following wetting by precipitation or irrigation, $K_{r,FAO}$ can be as high as 1. When the soil surface is dry, $K_{r,FAO}$ is small and can even reach zero. E is presumed to take place in two stages and the reduction coefficient $K_{r,FAO}$ is expressed differently for both stages (Figure 2): energy is the limiting factor of E during stage I (constant drying rate) and soil moisture is the limiting factor during stage II (falling drying rate). Stage I begins from D_e=0 and holds until D_e is equal to the readily evaporable water (REW) and where the soil moisture equals to a given critical soil moisture θ_{cr} (value when soil begins to resist to evaporation). In this stage, the soil surface remains wet and the evaporation rate is controlled by the energy available at the soil surface. Stage I holds until water cannot be transported to near surface as fast as the rate to supply the atmospheric demand. Here stage II begins (D_e exceeds REW).

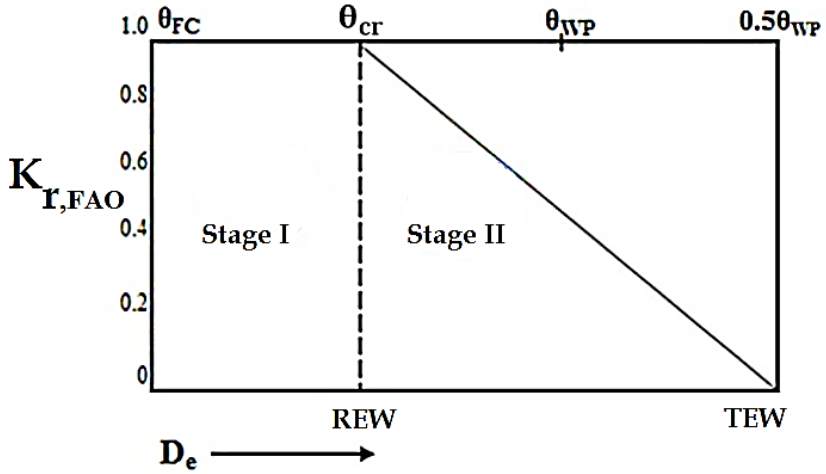

Figure 2: $K_{r,FAO}$ as function of De for classical FAO (Allen et al., 1998)

The reduction coefficient decreases and becomes smaller than 1 in proportion to the amount of water present in the surface soil layer. $K_{r,FAO}$ of Equation (5) is written as:

$$K_{r,FAO} = \frac{TEW - D_e}{TEW - REW} \quad ; D_e > REW \quad (6)$$

$$K_{r,FAO} = 1 \quad ; D_e < REW$$

with REW (mm) depending on soil texture. FAO-56 provides a table for each soil type. REW normally ranges from 5 to 12 mm and is highest for medium and fine textured soils (Ritchie, 1972; Ritchie et al., 1989). D_e is the cumulative depletion from the soil surface layer by evaporation (mm). The estimation of D_e requires a daily water balance model of the topsoil

253 layer. Otherwise soil moisture (θ_s) information can be used directly in the D_e calculation as
254 follows.

255 $$De = 1000(\theta_{FC} - \theta_s)Ze \quad (7)$$

256 TEW (mm) is the maximum depth of water evaporated from the surface layer:

257 $$TEW = 1000(\theta_{FC} - 0.5\theta_{WP})Ze \quad (8)$$

258 where Ze is the effective depth of soil in which the atmosphere can extract water by E.

259 θ_{FC}, θ_{WP} and REW are reported for each site in table 1 depending on the soil texture
260 classification. For Ze, FAO-56 recommended a value of 10 cm for coarse soils and 15 cm for
261 fine textured soils (Hanks and Hill, 1980; Ritchie, 1972; Wright, 1982). The values of TEW,
262 Z_e and REW are important factors that control and influence the E process.

263 Step calculation of the classical Kr_{FAO} evaporation model is presented in the flowchart (Figure
264 3).

265 3.2. New texture-based approach

266 The FAO-56 classical E method (Kr_{FAO}) is sensitive to the E depth. Thus, the FAO-2Kc E
267 equation uses a given soil thickness. In the FAO-2Kc, they recommended a value of Z_e of 0.1
268 to 0.15 m which is suitable for the water balance model. Jacquemin and Noilhan. (1990), Lee
269 and Pielke. (1992) and Noilhan and Planton. (1989) proposed a formulation of soil
270 evaporative efficiency based on surface soil moisture and soil moisture at the field capacity in
271 two specific soil thickness layers. Chanzy and Bruckler, (1993), Komatsu. (2003) and Merlin
272 et al. (2016, 2011) found a nonlinear behavior of soil evaporative efficiency as a function of
273 soil moisture.

274 Merlin et al. (2011) proposed an expression of the soil evaporative efficiency for various soil
275 thicknesses based on soil moisture and soil texture information. The reduction coefficient K_r
276 based on soil texture ($K_{r,text}$) is written as:

277 $$K_{r,text} = \left[0.5 - 0.5\cos\left(\frac{\pi\,\theta_s}{\theta_{max}}\right)\right]^P \;;\; \theta_s < \theta_{max} \quad (9)$$

278 $$K_{r,text} = 1 \;;\; \theta_s > \theta_{max}$$

where θ_s is the surface soil moisture, θ_{max} is taken equal to soil moisture at saturation θ_{SAT} by contrast of the work of Jacquemin and Noilhan. (1990) and Lee and Pielke. (1992), and P is a semi-empirical parameter depending on the soil moisture sensing depth and soil proprieties (texture).

Merlin et al. (2016) proposed an empirical Pedo-transfer (PTF) equation of the critical soil moisture ($\theta_{1/2}$) at which the actual E rate is half the potential E rate. In practice $\theta_{1/2}$ was correlated with soil texture (clay and sand content) with a good correlation coefficient (0.6 for sand fraction and 0.8 for clay fraction). A negative correlation was found between $\theta_{1/2}$ and sand fraction while it increases as a function of clay fraction. To benefit from the complementary information on soil water retention capacity, a multilinear regression of $\theta_{1/2}$ with both sand and clay fractions has been established named as the texture-based PTF. In this study, the PTF of Merlin et al. (2016), is used to check out its utility within the FAO formalism. This formulation is tested over 33 study sites to evaluate the FAO evaporation estimates, with 32 sites belonging to the calibration data set of Merlin et al. (2016) and the remaining site (MOBou) used as an independent data set for the evaluation of E estimates. Then, the three additional independent sites (EC1, EC2, B123) are used to assess wheat surface evapotranspiration. All the three sites were not used in the calibration process in Merlin et al. (2016).

$\theta_{1/2}$ is then written as:

$$\theta_{1/2} = 0.20 + 0.28 f_{clay} - 0.16 f_{sand} \qquad (10)$$

The advantage of the Eq 9, is that it can be calibrated using one single parameter P as shown in Merlin et al. (2011). Indeed, the formulation presented in Merlin et al. (2011) is a parsimonious formulation well adapted for parameterization with texture information. Hence, the idea is to parametrize simply $\theta_{1/2}$ presented in Equation (10) as a function of the single parameter P in which $K_{r,text}$ is approached linearly at the mid-value ($K_{r,text}\left(\theta_{1/2}\right) = 0.5$). Therefore, P parameter can be deduced at $\theta_s = \theta_{1/2}$ by inverting Eq 9:

$$P = \frac{\ln\left[K_{r,text}\left(\theta_{1/2}\right)\right]}{\ln\left[0.5 - 0.5\cos\left(\frac{\pi \frac{\theta_1}{2}}{\theta_{SAT}}\right)\right]} \qquad \text{where} \quad K_{r,text}\left(\theta_{1/2}\right) = 0.5 \quad (11)$$

The flowchart for E calculation using the new approach is also illustrated in Figure 3.

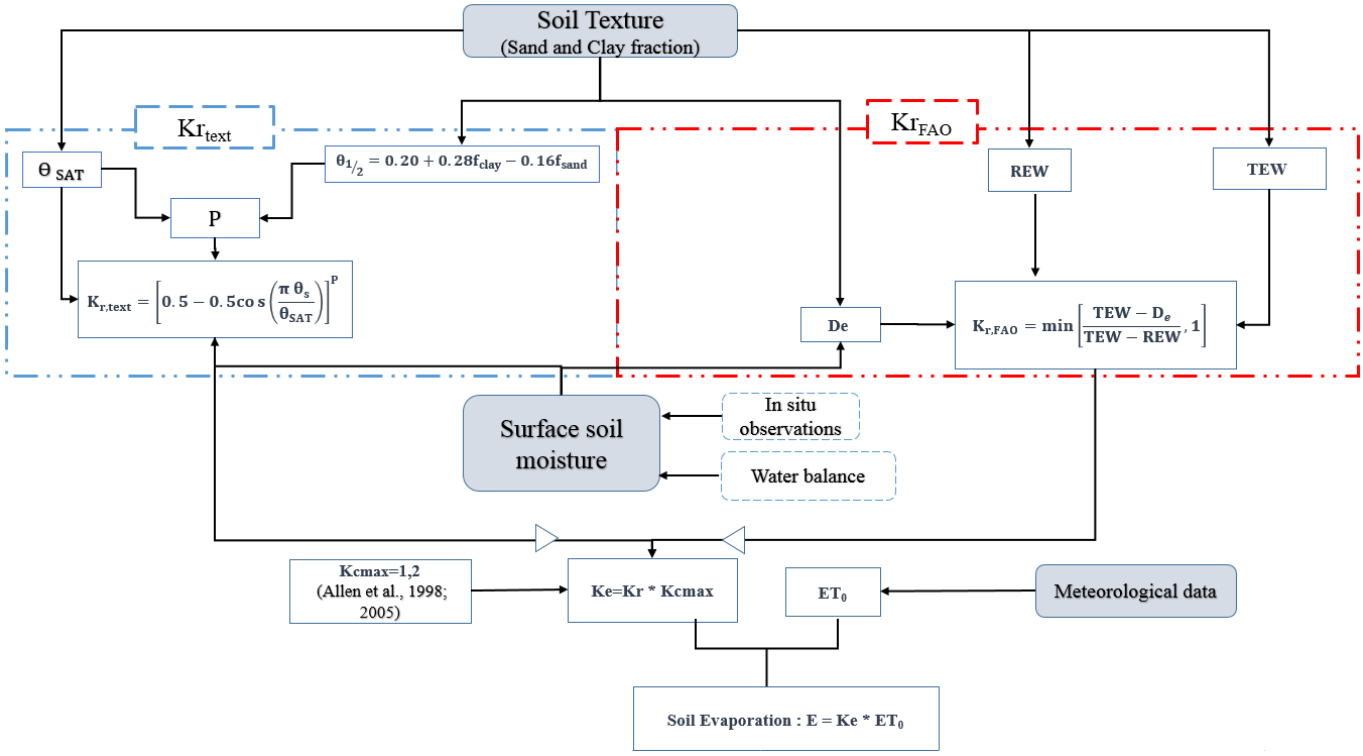

Figure 3: Flowchart presenting an overview of the main input and output data of the classical Kr_{FAO} (Em-dashed red rectangle) and the new textural-based approach Kr_{text} (Em-dashed blue rectangle) to estimate soil evaporation (E).

4. Results and discussions

Figure 4 plots the texture-based simulated Kr ($K_{r,text}$) as a function of soil moisture at 0-5 cm depth for all bare studied sites. Looking at the Figure 4, it can be observed that the $K_{r,text}$-θ_s relationship shows two different shape curves: The S-shaped curve and the Γ-shaped curve. The shape curves depend on the P value which is different for each site due to the soil texture information. For the 33 bare soil sites, the P values ranged from 0.24 to 2.46 from sandy ($\theta_{1/2,1}$) to clayey ($\theta_{1/2,2}$) soils, respectively. For fine textured soils $K_{r,text}$ increased rapidly with the increase of θ_s while $K_{r,text}$ increased slowlier for coarse texture soils. The same behavior was observed with physically-based simulated Kr in Chanzy and Bruckler. (1993). For P value higher than 0.5 the $K_{r,text}$ increases rapidly with θ_s. In this case the derivative of Kr with respect to θ_s is equal to zero at $\theta_s = 0$ and when θ_s reaches the saturation (θ_{sat}) $K_{r,text}$ equals 1. Contrarily, for the sites with a P value smaller than 0.5, the slope $\frac{\partial K_{r,text}}{\partial \theta}$ at $\theta_s = 0$ tends to infinity.

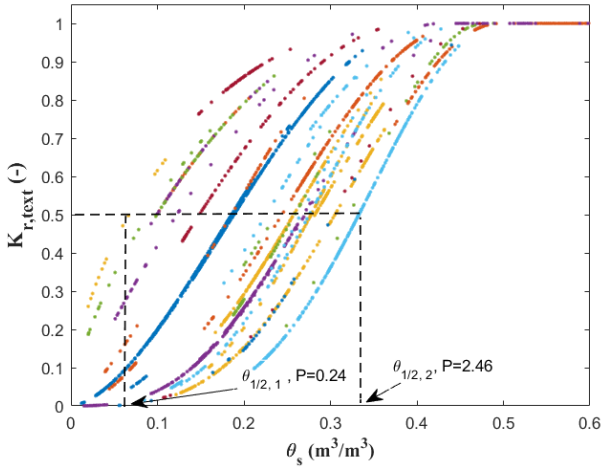

Figure 4: Texture-based K_r simulated by the new model as function of in situ surface soil moisture for the different 33 used sites. The very clayey soil and very sandy soil in our data set correspond to P values equal to 2.46 and 0.24, respectively.

4.1. Evaporation estimates over bare soils using observed soil moisture data

In this sub-section we present the performance of the texture-based ($K_{r,text}$) by implementing a pedo-transfer function developed in Merlin et al. (2016) within the FAO formalism and the FAO ($K_{r,FAO}$) classical evaporation model compared to E measurements for some sites where the measurements are available. The developed model was tested over different soil texture sites (covering the range of clayey, silty, sandy soil types). Both methods were tested using *in situ* soil moisture measured at 0-5cm soil depth as forcing. Figure 5 shows the performance of the two methodologies; classical FAO (E_{FAO}) and texture-based formulation (E_{New}) compared to measurements for different ranges of clay, sand and silt fractions: silty loam (DESeh, AUStu, BELon and ITCas), sandy loam (NISav, USMo1), Clay (MEYaq) loam (USDk1) and loamy sand (USMo7). Key statistical information about model performance are reported in Figure 6 for all study sites, such as root mean square error (RMSE), determination coefficient (R^2) and mean bias error (MBE).

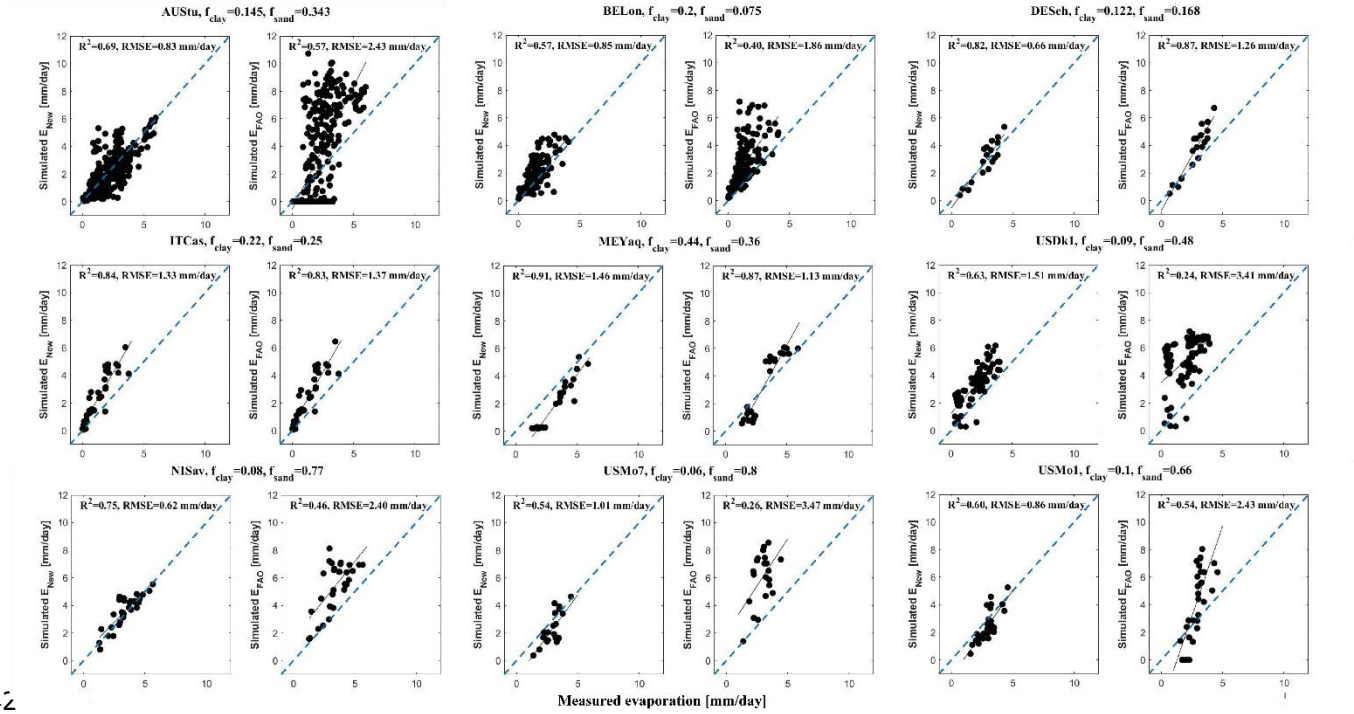

342

343 *Figure 5: Evaporation estimates from new model (E_{New}) and FAO-2Kc (E_{FAO}) using soil*
344 *moisture at 5-cm depth compared to measured evaporation.*

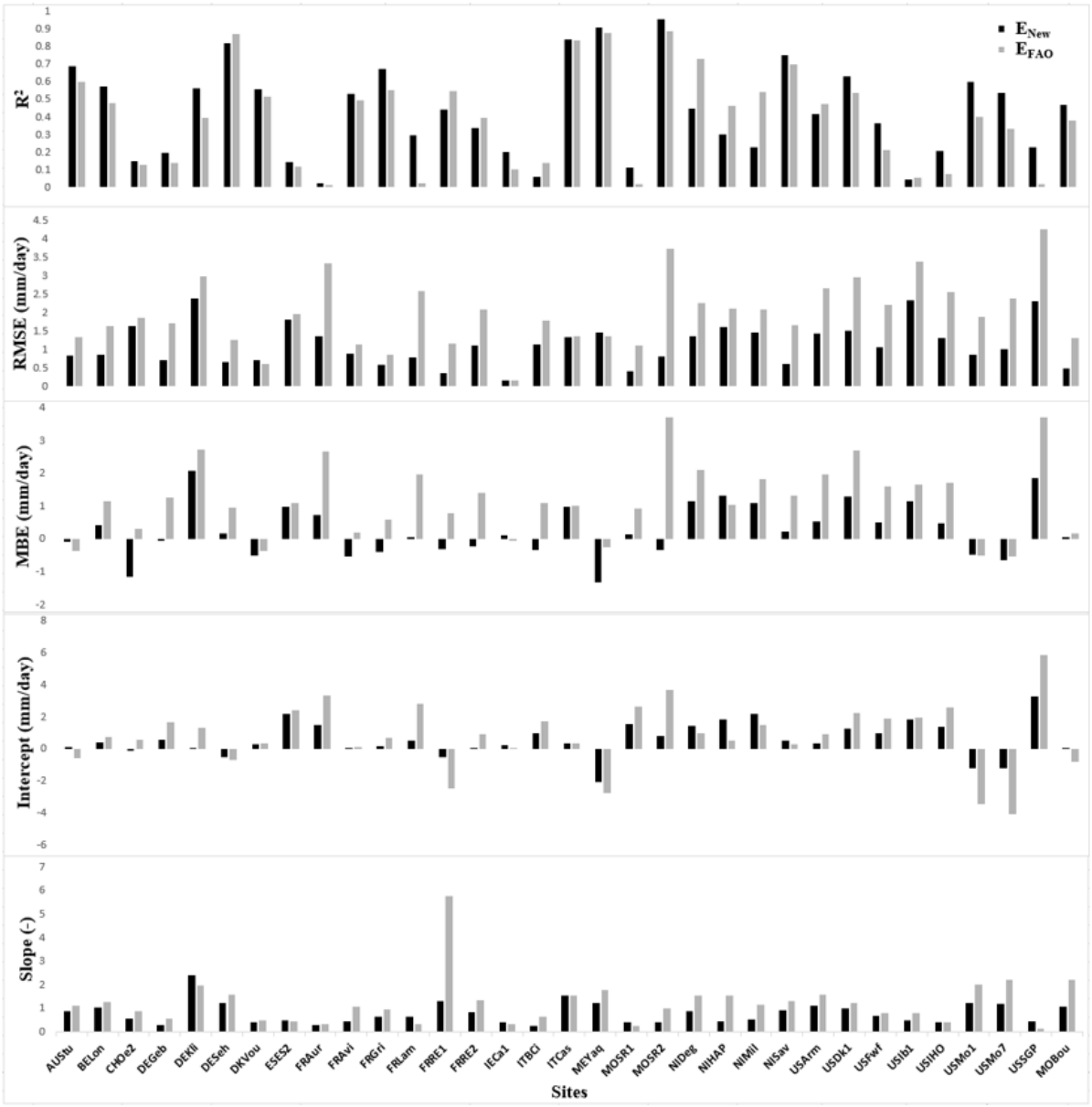

Figure 6: Bar graph of R^2, RMSE, MBE, intercept and slope of the linear regression between simulated and observed E using the Kr_{text} (black) and Kr_{FAO} (grey) for each site.

The scatter plot between observed and predicted E using the based-texture K_r (Figure 5) appears less dispersed around the 1:1 line compared to the classical Kr_{FAO}. Also, the bias is almost systematically reduced with the new texture-based formulation. A linear correlation is generally observed, which reveals that the new approach could be effective and successfully used to retrieve soil evaporation under different soil and climate conditions.

Although the statistical analyses provided relevant information about the effectiveness of the new developed model, statistical summary from Figure 6 revealed that the new K_r formalism has the capability to predict soil evaporation more accurately than the classical Kr_{FAO}. When

comparing the R^2, RMSE, MBE, slope and intercept for each site, one can observe that the performance of the new K_r based on soil texture information is better than the classical representation of K_r. By using the new formalism, an improvement of R^2 from 0.57, 0.40 and 0.46 to 0.69, 0.57 and 0.75 with a decrease of RMSE from 2.43, 1.86 and 2.40 mm/day to 0.83, 0.85 and 0.62 mm/day is obtained for AUStu, BELon and NISav sites, respectively. The texture-based $K_{r,text}$ appears to show its better performance for all soil types. For sandy loamy soil we reached an R^2 of 0.75 (0.60) and a RMSE of 0.62 mm/day (0.86) for the NISav (USMo1) site. For loamy sandy soil, R^2 reaches 0.54 with an RMSE equal to 1.01 mm/day for USMo7 site, while for clayey soil as we reached an R^2 of 0.96 and RMSE of 0.80 for MOSR2 site.

In some study sites, even if the new approach still provides better results, a relatively poor performance may occur for both approaches, (eg. USIb1, FRAur and CHOe2 sites). The relatively poor results obtained at those sites are not due to the model itself but might be due to the collected true measurements. As indicated in Merlin et al. (2016) most of the study sites were not in a fully bare soil condition, as these sites were cropped and a selection of the periods when soil is quasi bare was investigated, assuming no crop (no transpiration) over the sites. This assumption could be a source of errors and could degrade the data quality. In addition, soil depth could impact the results and could generate some uncertainties. To assess the impact of the soil depth on the proposed approach, a sensitivity analysis is carried out by using soil moisture at 0-10 cm depth. Overly, the new textural based Kr provides more accurate results than the $K_{r,FAO}$. This is due to its physical basis, given that the $K_{r,text}$ is implemented in a phenomenological model based on observational data, while the $K_{r,FAO}$ was mainly built on ad hoc assumptions. Lehmann et al. (2018) showed the importance of soil texture on the variation of surface evaporation as a function of soil moisture content. Moreover, as cited in Merlin et al. (2016) and Wetzel and Chang (1988), the nonlinear relationship between soil evaporation and soil moisture varied systematically with soil properties. In addition, the critical soil moisture content where the evaporation rate drops below potential rate, was related to soil texture through the field capacity (Budyko, 1956; Manabe, 1969). Through the new $K_{r,text}$, we succeeded in introducing the effect of soil texture on E rate, which is not taken into account properly in other land surface models (Phillips et al., 2017).

4.2. Sensitivity of Kr formulations to the thickness of surface soil layer

In this study the E estimates is assessed using soil moisture data at shallow depths near the soil surface (0-5 cm and 0-10 cm depending on the site). As a prospect to integrate $K_{r,text}$ in the FAO-2Kc (next sub-section), which uses a surface soil thickness (Z_e) of either 10 or 15 cm, we need to assess the applicability of the $K_{r,text}$ to the 0-15 cm soil layer. This is more crucial as all soil evaporation formulations are sensitive to the thickness of the surface soil layer (Merlin et al., 2011). Therefore, a sensitivity analysis has been made to quantify the impact of active soil evaporation depth to E as well as the integration of the new $K_{r,text}$ into the FAO-2Kc formulation. This was made for both approaches using 0-10 cm (in replacement of the 0-5 cm) collected soil moisture. Note that, only the sites where soil moisture data at 10 cm were available have been used for the sensitivity analysis. Figure 7 presents the simulated soil E using texture-based Kr_{text} and classical Kr_{FAO} compared to *in-situ* measurements for the 0-10 cm soil moisture depth. Due to the non-availability of soil moisture at 10 cm depth for all sites, eleven sites were selected to test the new approach where soil moisture data at 10 cm depth were available. Figure 7 shows the simulated evaporation using both classical Kr_{FAO} and new model Kr_{text} compared to *in situ* measurements for six sites with different soil textures and climate conditions: clayey (MOBou, MEYaq), silty loam (BELon, FRGri, DESeh) and sandy loam (IECa1). Figure 8 presents the performance of the approaches over all the eleven study sites.

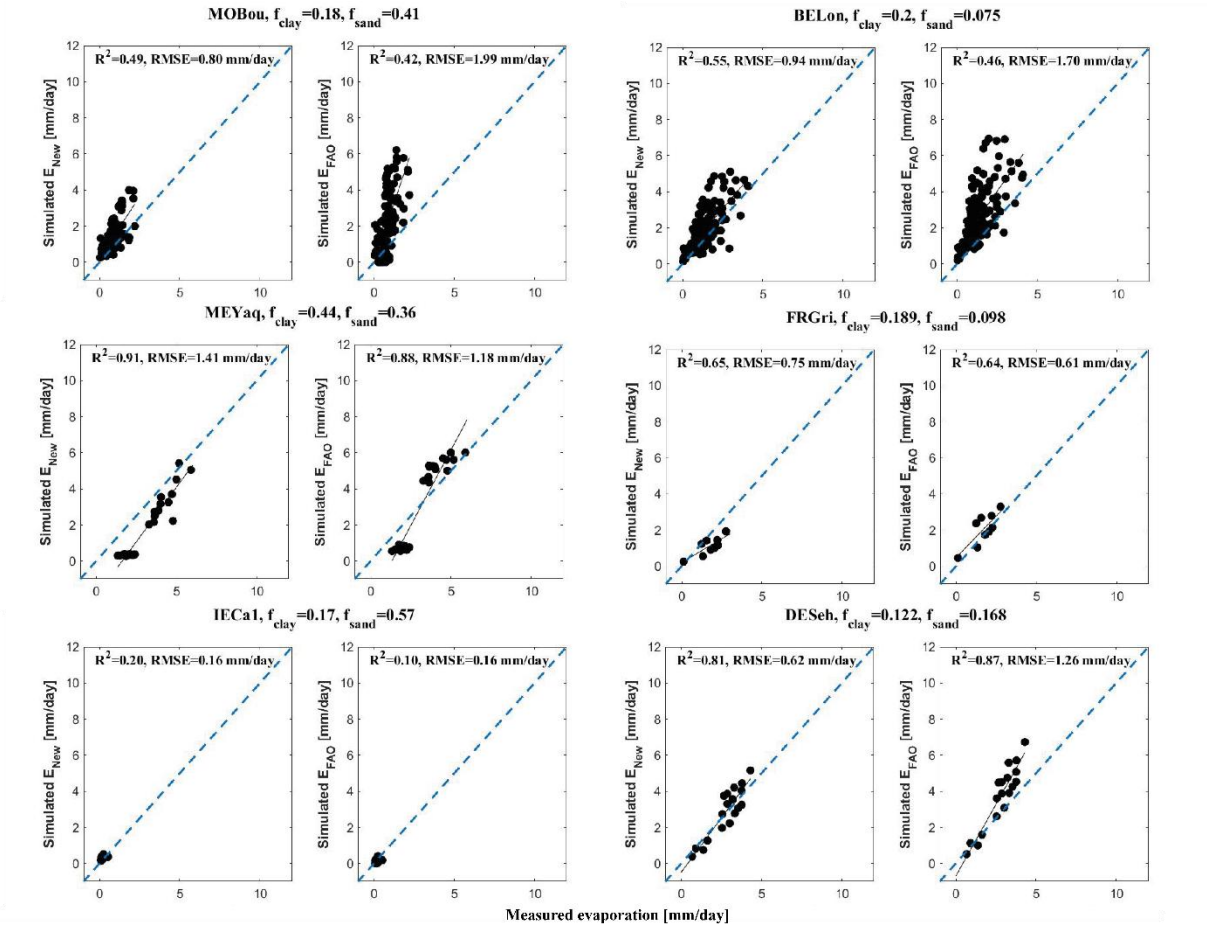

406

407 *Figure 7: Evaporation estimates from new model (E_{New}) and Kr_{FAO} (E_{FAO}) using soil moisture*
408 *at 10 cm depth compared to measured evaporation.*

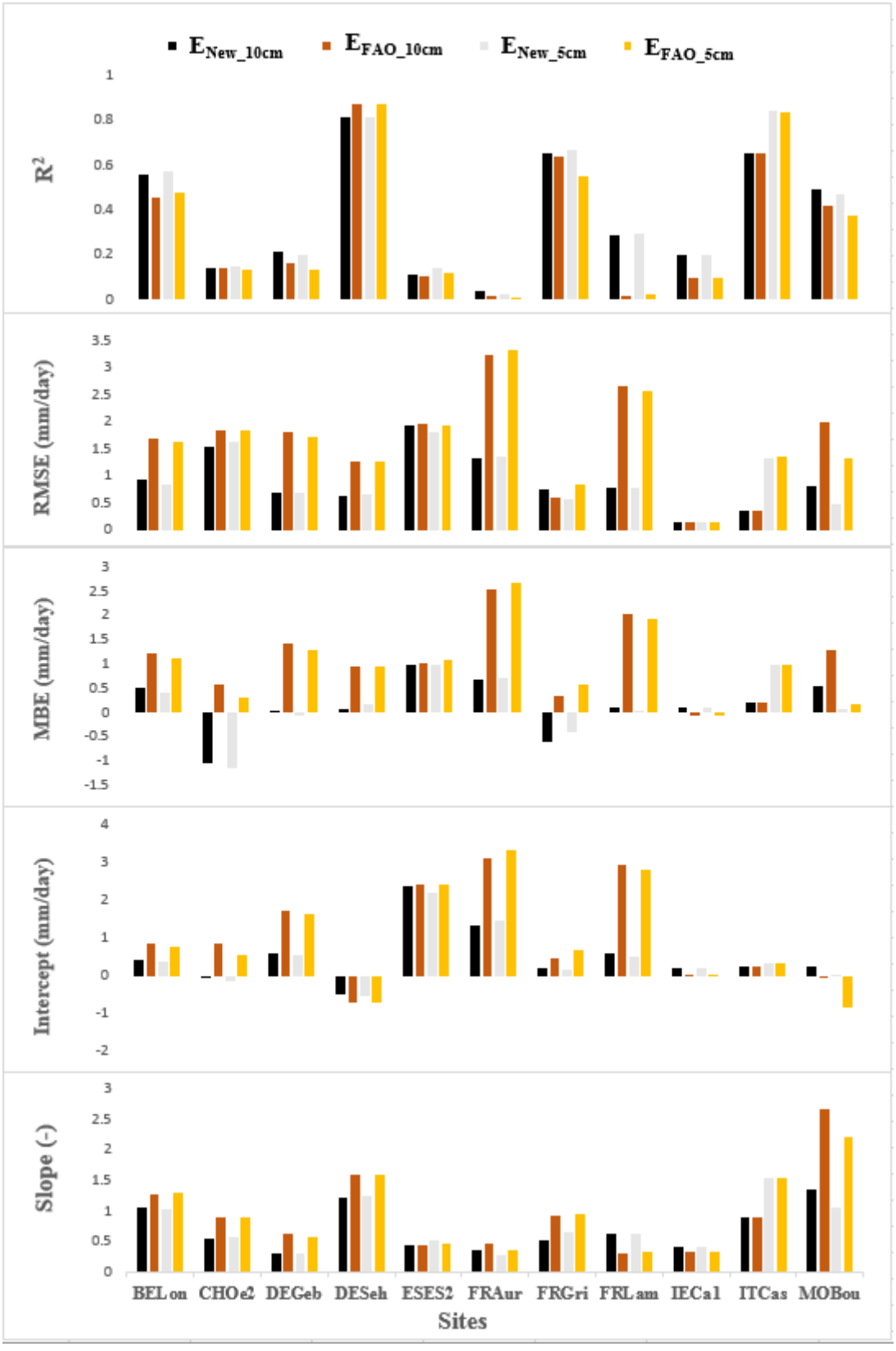

Figure 8: Bar graph of the statistical parameters (R^2, RMSE, MBE), the intercept and slope of the linear regression between simulated and observed E using the new texture-based (black '5cm', grey '10 cm') and Kr_{FAO} (Brown '5cm', orange '10 cm') for each site. 5 cm and 10 cm are the soil depths.

Looking at the results in Figures 7 and 8, generally the new textural-based model captures well the variation of evaporation measurements. Mostly the new model provides a more accurate prediction of E all over the 11 study sites. The new model shows its capabilities to solve the common overestimation problem that occurs especially under arid and semi-arid conditions (Michel et al., 2016) as shown at sites MOBou, BELon and DESeh. The new model yielded lower RMSEs over almost all sites in comparison with classical Kr_{FAO}, with a value of 0.94 mm.day^{-1} and 1.70 mm.day^{-1}, respectively, at BELon site as an example.

The statistical results are presented in Figure 8, showing the performance of both approaches (classic Kr_{FAO} and new texture-based Kr_{text}) using soil moisture data at 0-5 cm and 0-10 cm depth. In same sites, it appears from the statistical results that the performance of the new approach slightly decreases while the classical Kr_{FAO} slightly improves providing better results by using soil moisture at 0-10 cm instead of 0-5 cm depths. However, the new approach still outperformed the Kr_{FAO} approach regardless of the sensing depth (0-5 or 0-10 cm) of the soil moisture measurements. The error between Kr_{FAO} and *in-situ* evaporation measurements is slightly reduced when using soil moisture at 0-10 cm instead of 0-5 cm depths, from 0.85 to 0.60 mm.day^{-1} while by using new model the error is slightly increased from 0.58 to 0.75 mm.day^{-1} over FRGri site. The improvement of the performance of Kr_{FAO} approach by using soil moisture at 0-10 cm instead of soil moisture at 0-5cm, is due to the fact that the evaporation process can occur from deeper layers than the 0-5 cm layer. This is especially occurred in arid and semi-arid areas in which the FAO-2Kc recommends the use of a layer of 0-15 cm. Similarly, the new formulation of the evaporation reduction factor is intrinsically dependent on the soil moisture measurements depth. It is reminded that the used formulation has been developed and calibrated using a 0-5 cm soil layer. As stated by Merlin et al. (2011), the P value is an increasing function of the soil depth for a given soil moisture value. This could be responsible for the slight underestimation of new model when using the 0-10 cm layer. However, the Kr_{FAO} formulation is generally based on moisture data from 0 to 15 cm (Allen, 2000). The sensitivity analysis shows that the new approach generally outperformed the classical Kr_{FAO} at either 5cm or 10 cm soil depths.

4.3. Coupling the $K_{r,text}$ model with the FAO crop water budget model: application to wheat cropped fields

As mentioned above, the main objective is to improve the soil evaporation estimates through using a formulation of Kr based on soil texture information and soil moisture estimates. The

point is that retrieving soil evaporation is more relevant over bare soils and sparse areas. However, over cropped area, retrieving surface evapotranspiration is more important. For this reason, as a source of validating of our approach, we tested the new textural-based Kr approach over the cropped fields defined before: B123 (2002-2003), EC1 and EC2 (2016-2017). Two cases were tested for each approach, where the soil evaporation component is forced by i) *in-situ* soil moisture θ_s, using the classical FAO-2Kc ($E_{FAO}+\theta_s$) or the new approach ($E_{New}+\theta_s$) and ii) simulated soil moisture from the water balance (θ_{FAO}), for classical FAO-2Kc and new approach termed in the plots as ($E_{FAO}+\theta_{FAO}$) and ($E_{New}+\theta_{FAO}$), respectively.

In order to observe the response of the evaporation coefficients to water supply, Figure 9 shows the temporal variation of Kr for FAO-2Kc ($K_{r,FAO}$) and new textural-based Kr ($K_{r,text}$) approaches for the cropped fields.

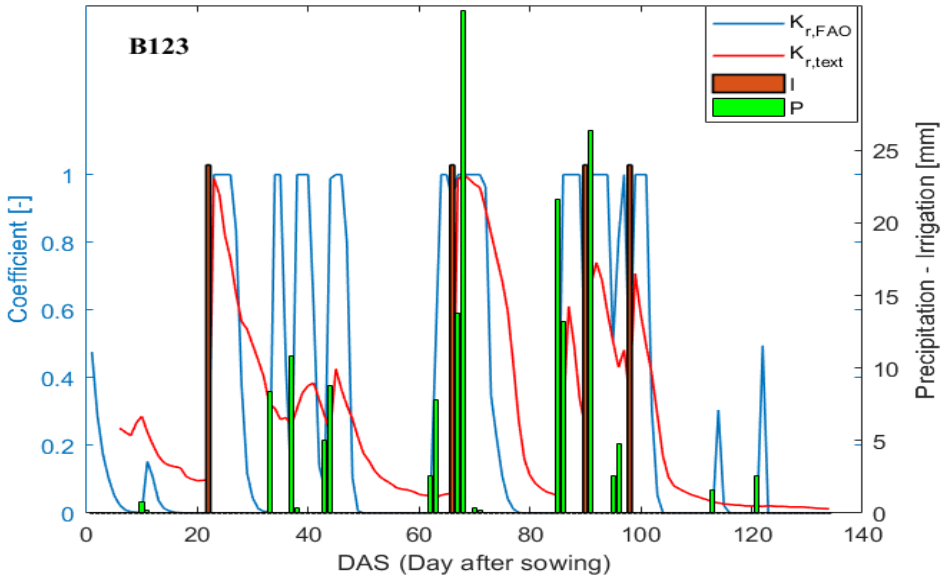

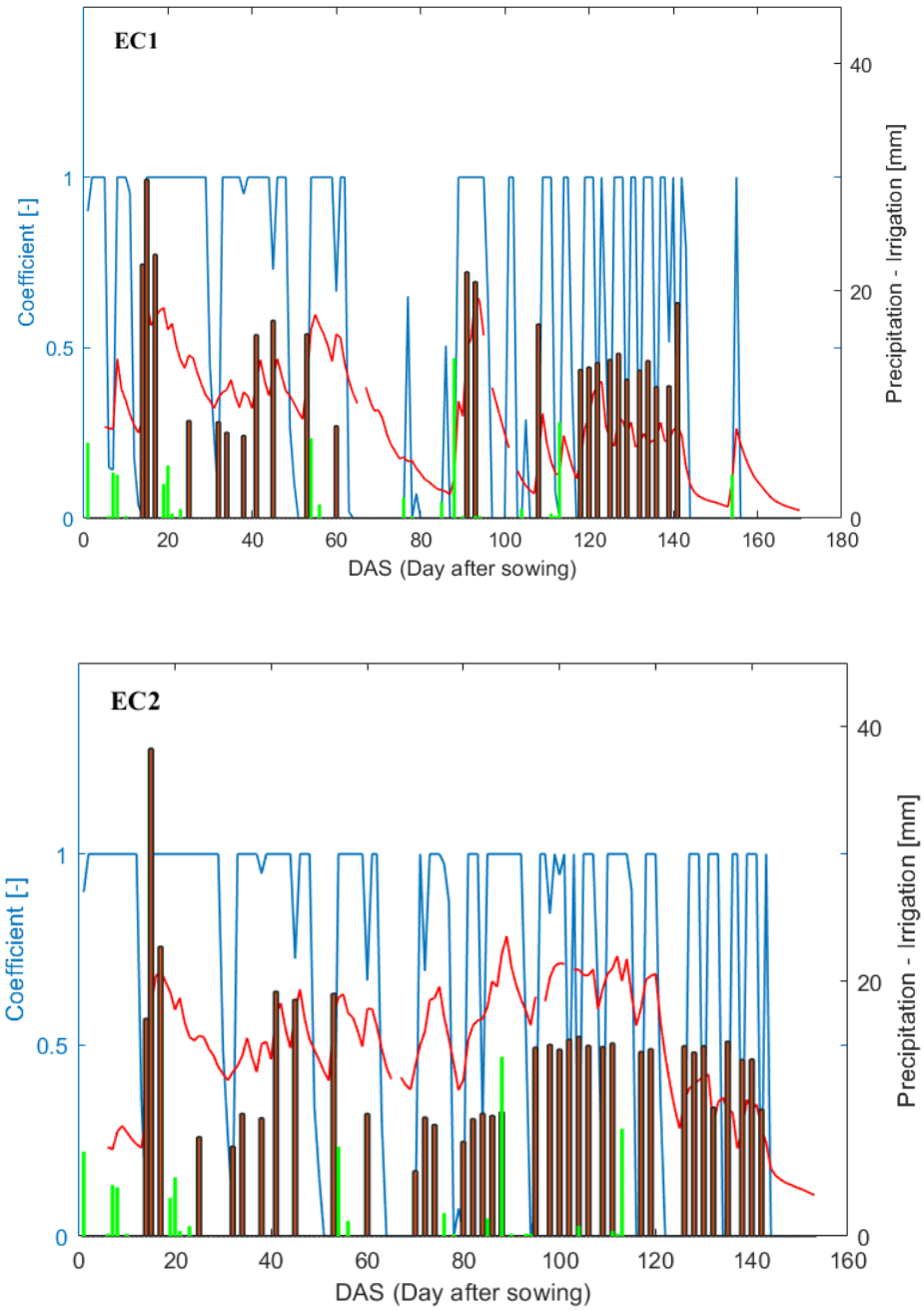

Figure 9: Time variation of the K_r estimated from FAO-2Kc ($K_{r,FAO}$) and new textural based Kr ($K_{r,text}$) for the studied fields.

From the Figure 9, it can be observed that at the initial stage of crop growth, the $K_{r,FAO}$ values are high and reach its maximal value (1). This is due to the small fraction of soil surface covered by wheat crop. In addition, following rain or irrigation both Kr increase, while the Kr is small and can reach zero in the drier periods when the soil resistance to evaporation increases.

Overall, $K_{r,text}$ detects soil stress periods and responds well to the water supplied by precipitation or/and irrigation. After an irrigation or precipitation event both Kr increase with different amplitudes. The new textural-based Kr appears to be more physical than the $K_{r,FAO}$. It consistently increases following the supplied water amounts and then gradually decreases. This is not the case for $K_{r,FAO}$, which increases and decreases rapidly. This is due to the response and the soil drying time which is well taken into account in the $K_{r,text}$ approach. Especially in stage 2 when soil moisture is the limiting factor, the $K_{r,text}$ decreases progressively for each soil type depending on the soil properties.

An increase of Kr comes with an increase of the evaporation rate after a water supply by irrigation or/and rain. Consequently, soil evaporation losses are considerable. Figure 10 presents a daily evolution comparison of the measured ET (ET_{obs}) with simulated ET using standard FAO-2Kc ($E_{FAO}+\theta_{FAO}$) and new approach ($E_{New}+\theta_{FAO}$). Soil evaporation and wheat transpiration were also presented in the same figure for the three studied fields.

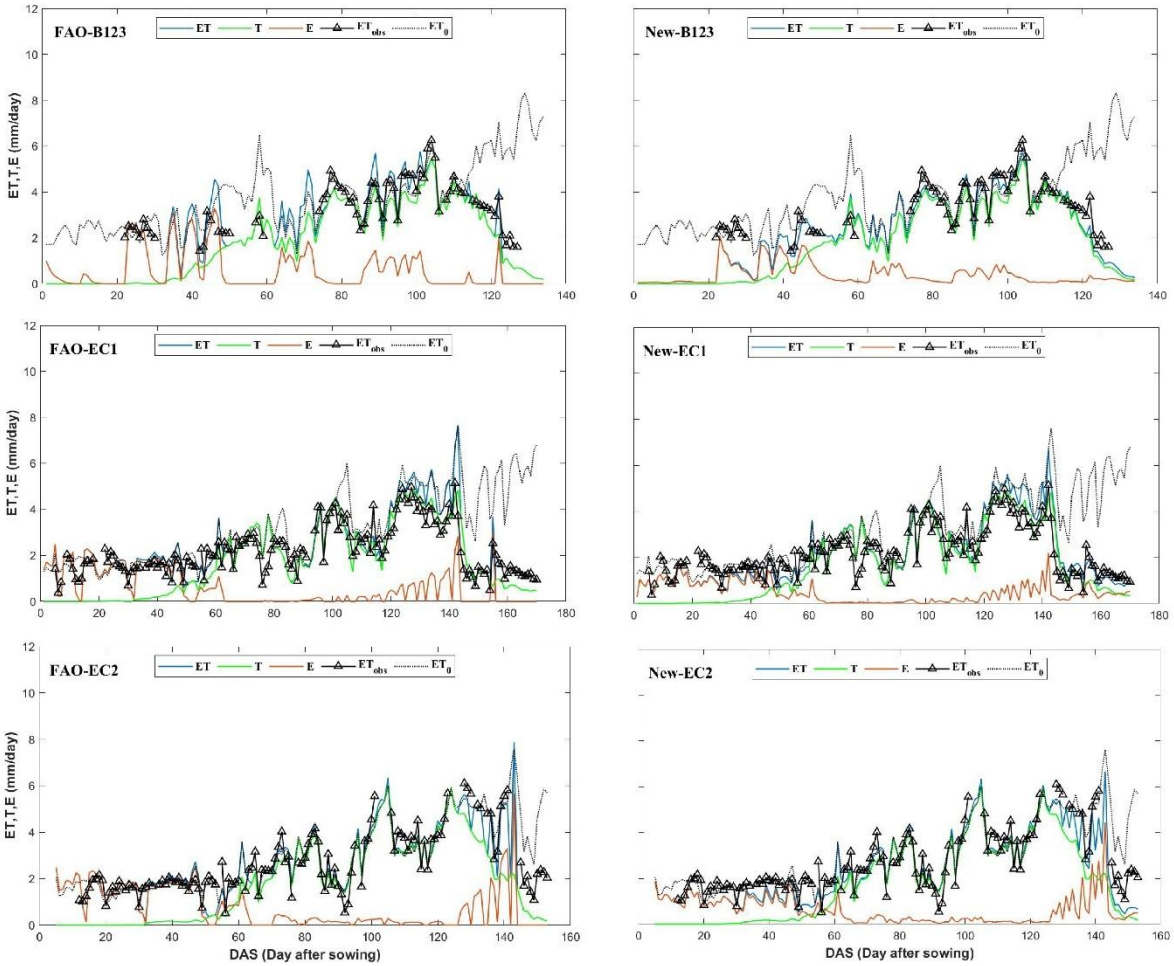

Figure 10: Time series comparison of daily plant transpiration (T), soil evaporation (E), ET_0 as well as the ET observed by EC (ET_{obs}) and simulated by FAO-2Kc (left) and new model (right) over the study fields.

According to figure 10, we notice that the new approach follows correctly the measured ET. As it is seen, the new formulation of E helps catch the variation of surface ET especially at the beginning and the end of the season when ET is dominated by E and when transpiration is relatively small. This behavior of the classical FAO-2Kc was also reported in Rafi et al. (2019), where the classical FAO was found to underestimate E leading to an underestimation of ET especially during the senescence period. While in Olivera-Guerra et al. (2018) an overestimation issue was observed using thermal-derived E estimates. Using soil moisture and texture information lead to a correction of E in the initial and late stage. To evaluate visually and quantitatively the used approaches, the predicted ET were plotted against the observed ET (ET_{EC}) and are presented in Figure 11 for the three wheat crop fields.

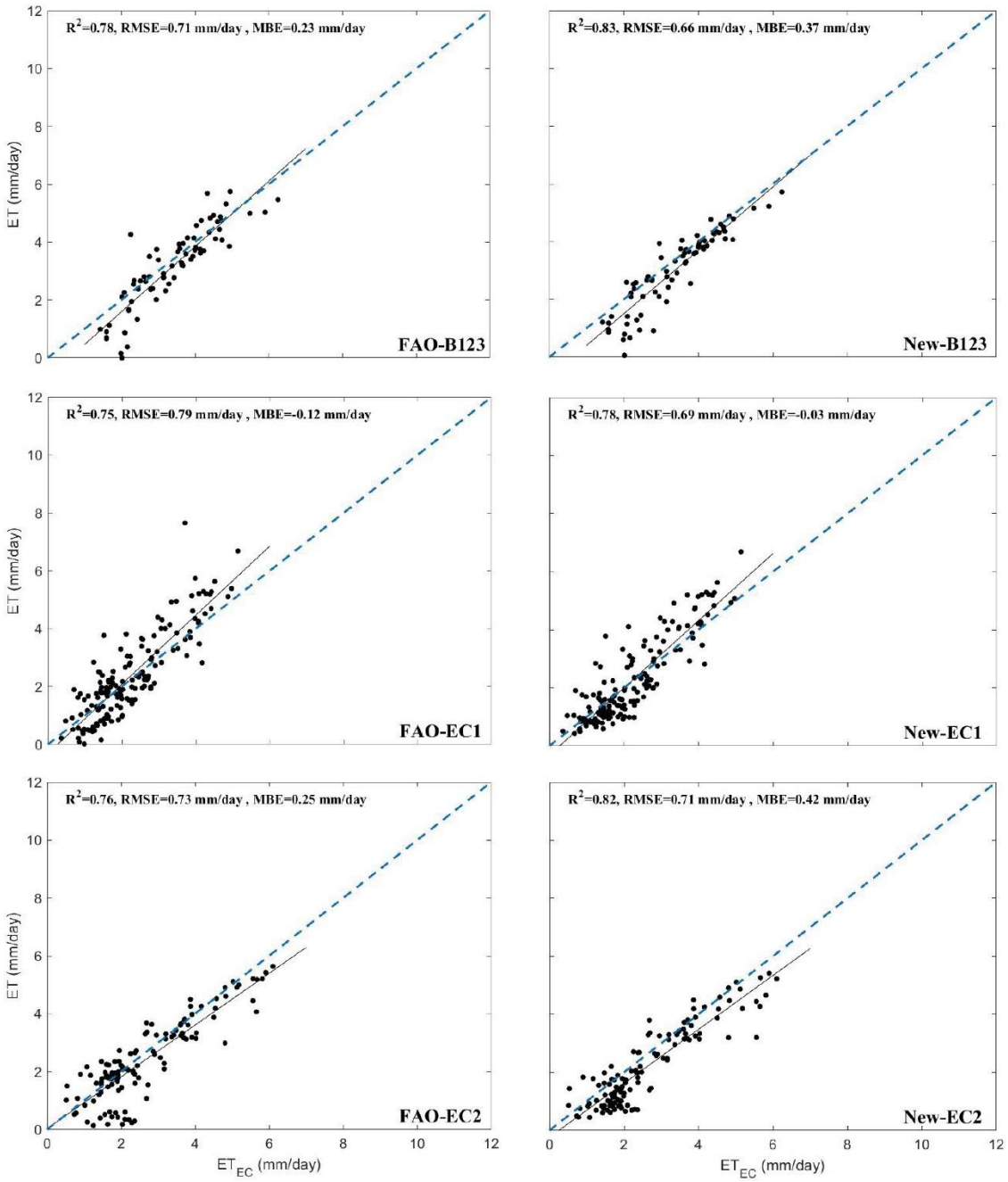

Figure 11: Scatterplot of simulated ET-FAO using the FAO-2Kc (left plot) and the new model forced by simulated soil moisture (θ_{FAO}) (right plot) versus Eddy covariance ET (ET_{EC}) over the B123, EC1 and EC2 study fields.

From the statistical results presented in Figure 11, the new method provides the best results in term of accuracy and stability over the three wheat crop fields. The ET is estimated with an RMSE equal to 0.71 and 0.66 mm/day and an R^2 equal to 0.78 and 0.83 by using the classical FAO-2Kc and the proposed method for B123 field, respectively. An improvement is observed when using the new method. This is especially seen for small values of ET where the estimations are less scattered around the 1:1 line.

Statistics of the studied four cases are shown and reported in Figure 12. Using in situ soil moisture or simulated θ_s from water balance in the new model gives almost the same results. A slight difference is observed in the statistical results in terms of RMSE and R^2. The E_{New}+θ_s shows the best results compared to the other methods with the lowest RMSE (0.55 mm/day) and the highest R^2 of about 0.84 in the B123 field. The reason behind the good results when *in-situ* soil moisture was used is the fact that soil moisture is directly measured using TDR sensors while the simulated soil moisture is estimated using water balance equation where errors can accumulate from each water balance components. However, the classical approach shows good results compared to new approach in the EC2 field, although the difference between both approaches is smaller.

Overly, results showed that the new textural approach for E provided more accurate results in terms of ET regardless of the source (direct measurements and model simulations) of soil moisture estimates.

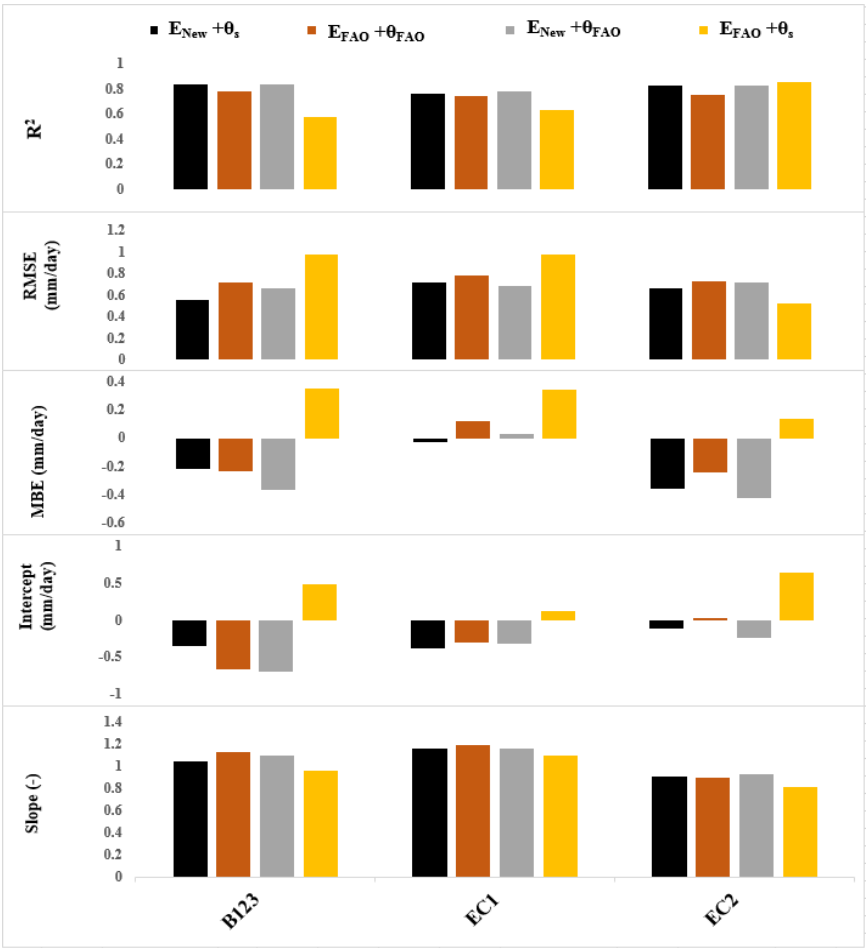

Figure 12: Bar graph of R^2, RMSE, MBE, intercept and slope of the linear regression between simulated and observed ET using the 4 approaches.

5. Conclusion

This work aims to improve the representation of the soil evaporation (E) component of the total evapotranspiration (ET). In the classical FAO-2Kc, the evaporation reduction coefficient Kr is estimated based on an ad-hoc relationship with soil texture. This standard formulation provides some limitation to quantify the E process. Rafi et al. (2019) and Olivera-Guerra et al. (2018) reported that the standard FAO-2Kc overestimates or underestimates E in the beginning or/and the end of the agricultural season.

A new E formulation is developed by including the soil texture information into Kr. The idea here is to adapt the Kr representation to the nonlinear relationship between soil moisture and E in a range of soil texture types and surface conditions as in Merlin et al. (2016a, 2018). By including the new formulation into the FAO-2Kc the typical drying process is modified. The new evaporation formulation was tested over 33 bare soil sites distributed all over the world. The sites are different in term of soil texture and meteorological conditions. Soil moisture measurements at 0-5cm and 0-10 cm were used to further assess the impact of soil measurement depths on the E rate. FAO-2Kc and the new texture-based approach were evaluated by comparing them against in situ E measurements. From the obtained results, the new approach provides the best results in term of accuracy and robustness. The new model provided solid basis for describing the soil texture impact on the E reduction coefficient. However, some uncertainties were observed, and this could be due to the water diffusion flux which is not taken into account in the FAO-2Kc model and represents the soil as a simple reservoir. Further, the new evaporation model was evaluated over a 3 monitored wheat cropped fields, where evapotranspiration is retrieved. The simulated evapotranspiration was compared to eddy covariance measurements installed in the 3 sites. A comparison of the 4 cases is investigated by using both standard FAO-2Kc and the new approach. Each model is forced by soil moisture either measured in situ or simulated by the water balance model. Results showed that the texture-based approach provides the best results with low errors over the studied sites using field-scale measurements data.

To cope with some limitations of FAO-2Kc model, remote sensing data can be assimilated (Amazirh et al., 2021, 2018). However, the use of remote sensing data in the FAO-2Kc would require a match between the soil layers represented by the model and the sensing depth of spaceborne observations. The point is that the sensed thickness of remote sensing data rarely exceeds 0-5 cm. In this vein, coupling the FAO-2Kc with remote sensing data will be an asset for minimizing modeling errors, and for better constraining the ‘often unavailable over most

irrigated area' irrigation input data. To do this, changing the depth of the top-soil layer represented by the FAO-2Kc model to fit with the near-surface soil moisture derived from remote sensing is needed.

Acknowledgements

This study was conducted within the Center of remote sensing applications, at the Mohammed VI university-Morocco and was funded by the European Commission Horizon 2020 Programme for Research and Innovation (H2020) in the context of the Marie Sklodowska-Curie Research and Innovation Staff Exchange (RISE) action (REC project, grant agreement no: 645642), followed by ACCWA project, grant agreement no. 823965). The *in situ* data set was provided by the Joint International Laboratory TREMA (http://trema.ucam.ac.ma), the European Fluxes Database Cluster (http://www.europe-fluxdata.eu), the AmeriFlux sites, OzFlux site, long term observatories (AMMA, HOBE and SudMed), and the short term intensive field campaigns (EFEDA, ReSeDa, Yaqui'08, HAPEX-Sahel, IHOP, Monsoon'90 and SGP'97). The French Agence Nationale de la Recherche (MIXMOD-E project, ANR- 13-JS06-0003-01) is also acknowledged for extracting and pre-processing the bare soil evaporation database.

References

Ait Hssaine, B., Merlin, O., Rafi, Z., Ezzahar, J., Jarlan, L., Khabba, S., Er-Raki, S., 2018. Calibrating an evapotranspiration model using radiometric surface temperature, vegetation cover fraction and near-surface soil moisture data. Agricultural and Forest Meteorology 256–257, 104–115. doi:10.1016/j.agrformet.2018.02.033

Allen, R.G., 2000. Using the FAO-56 dual crop coefficient method over an irrigated region as part of an evapotranspiration intercomparison study. Journal of Hydrology 229, 27–41. doi:10.1016/S0022-1694(99)00194-8

Allen, R.G., Pereira, L.S., Raes, D., Smith, M., 1998. Crop evapotranspiration - Guidelines for computing crop water requirements - FAO Irrigation and drainage paper 56, Irrigation and Drainage. doi:10.1016/j.eja.2010.12.001

Allen, R.G., Pereira, L.S., Smith, M., Raes, D., Wright, J.L., 2005a. FAO-56 Dual Crop Coefficient Method for Estimating Evaporation from Soil and Application Extensions. Journal of Irrigation and Drainage Engineering 131, 2–13. doi:10.1061/(ASCE)0733-9437(2005)131:1(2)

Allen, R.G., Pruitt, W.O., Wright, J.L., Howell, T.A., Ventura, F., Snyder, R., Itenfisu, D., Steduto, P., Berengena, J., Baselga, J., Smith, M., Pereira, L.S., Raes, D., Perrier, A., Alves, I., Walter, I., Elliott, R., 2005b. A recommendation on standardized surface resistance for hourly calculation of reference ET o by the FAO56 Penman-Monteith method. doi:10.1016/j.agwat.2005.03.007

Amazirh, A., Chehbouni, A., Ojha, N., Rivalland, V., Merlin, O., Er-Raki, S., 2021. Improving FAO-56 estimates of ET in semi-arid region through combined assimilation of SMAP based disaggregated soil moisture and Landsat Surface Temperature. AFM.

Amazirh, A., Er-Raki, S., Chehbouni, A., Rivalland, V., Diarra, A., Khabba, S., Ezzahar, J., Merlin, O., 2017. Modified Penman–Monteith equation for monitoring evapotranspiration of wheat crop: Relationship between the surface resistance and remotely sensed stress index. Biosystems Engineering 164, 68–84.

599 doi:10.1016/j.biosystemseng.2017.09.015
600 Amazirh, A., Merlin, O., Er-Raki, S., 2019. Including Sentinel-1 radar data to improve the
601 disaggregation of MODIS land surface temperature data. ISPRS Journal of
602 Photogrammetry and Remote Sensing 150, 11–26. doi:10.1016/j.isprsjprs.2019.02.004
603 Amazirh, A., Merlin, O., Er-Raki, S., Gao, Q., Rivalland, V., Malbeteau, Y., Khabba, S.,
604 Escorihuela, M.J., 2018. Retrieving surface soil moisture at high spatio-temporal
605 resolution from a synergy between Sentinel-1 radar and Landsat thermal data: A study
606 case over bare soil. Remote Sensing of Environment 211, 321–337.
607 doi:10.1016/j.rse.2018.04.013
608 Anderson, R.G., Alfieri, J.G., Tirado-Corbalá, R., Gartung, J., McKee, L.G., Prueger, J.H.,
609 Wang, D., Ayars, J.E., Kustas, W.P., 2017. Assessing FAO-56 dual crop coefficients
610 using eddy covariance flux partitioning. Agricultural Water Management.
611 doi:10.1016/j.agwat.2016.07.027
612 Aouade, G., Ezzahar, J., Amenzou, N., Er-Raki, S., Benkaddour, A., Khabba, S., Jarlan, L.,
613 2016. Combining stable isotopes, Eddy Covariance system and meteorological
614 measurements for partitioning evapotranspiration, of winter wheat, into soil evaporation
615 and plant transpiration in a semi-arid region. Agricultural Water Management.
616 doi:10.1016/j.agwat.2016.07.021
617 Ayyoub, A., Er-Raki, S., Khabba, S., Merlin, O., Ezzahar, J., Rodriguez, J.C., Bahlaoui, A.,
618 Chehbouni, A., 2017. A simple and alternative approach based on reference
619 evapotranspiration and leaf area index for estimating tree transpiration in semi-arid
620 regions. Agricultural Water Management 188, 61–68. doi:10.1016/j.agwat.2017.04.005
621 Balwinder-Singh, Eberbach, P.L., Humphreys, E., Kukal, S.S., 2011. The effect of rice straw
622 mulch on evapotranspiration, transpiration and soil evaporation of irrigated wheat in
623 Punjab, India. Agricultural Water Management 98, 1847–1855.
624 doi:10.1016/j.agwat.2011.07.002
625 Boast, C.W., Robertson, T.M., 1982. A "Micro-Lysimeter" Method for Determining
626 Evaporation from Bare Soil: Description and Laboratory Evaluation. Soil Science
627 Society of America Journal 46, 689–696.
628 doi:10.2136/sssaj1982.03615995004600040005x
629 Brisson, Perrier, 1991. A semi-empirical model of bare soil evaporation for crop simulation
630 models. Water resources 27, 719–727.
631 Budyko, M.I., 1956. Heat balance of the Earth's surface. Gidrometeoizdat, Leningrad. Cahill,
632 255.
633 Chanzy, A., Bruckler, L., Evaporation, S., 1993. Significance of Soil Surface Moisture With
634 Respect to Daily Bare Soil Evaporation. Water Resources Research 29, 1113–1125.
635 doi:10.1029/92WR02747
636 Chehbouni, A., Escadafal, R., Duchemin, B., Boulet, G., Simonneaux, V., Dedieu, G.,
637 Mougenot, B., Khabba, S., Kharrou, H., Maisongrande, P., Merlin, O., Chaponnière, A.,
638 Ezzahar, J., Er-Raki, S., Hoedjes, J., Hadria, R., Abourida, A., Cheggour, A., Raibi, F.,
639 Boudhar, A., I.Benhadj, Hanich, L., Benkaddour, A., Guemouria, N., Chehbouni, A..,
640 Lahrouni, A., Olioso, A., Jacob, F., Williams, D.G., Sobrino, J. a, 2008. An Integrated
641 Modelling and Remote Sensing Approach for Hydrological Study in Arid and Semi-arid
642 Regions: The SUDMED Programme. International Journal of Remote Sensing 29, 5161–
643 81.
644 Cosby, B.J., Hornberger, G.M., Clapp, R.B., Ginn, T.R., 1984. A Statistical Exploration of the
645 Relationships of Soil Moisture Characteristics to the Physical Properties of Soils. Water
646 Resources Research 20, 682–690. doi:10.1029/WR020i006p00682
647 Debnath, S., Adamala, S., Raghuwanshi, N.S., 2015. Sensitivity Analysis of FAO-56
648 Penman-Monteith Method for Different Agro-ecological Regions of India.

649 Environmental Processes 2, 689–704. doi:10.1007/s40710-015-0107-1
650 Diarra, A., Jarlan, L., Er-Raki, S., Le Page, M., Aouade, G., Tavernier, A., Boulet, G.,
651 Ezzahar, J., Merlin, O., Khabba, S., 2017. Performance of the two-source energy budget
652 (TSEB) model for the monitoring of evapotranspiration over irrigated annual crops in
653 North Africa. Agricultural Water Management 193, 71–88.
654 doi:10.1016/j.agwat.2017.08.007
655 Doorembos, J.&, Pruitt, W.O., 1975. Guidelines for Predicting Crop Water Requirements.
656 FAO Irrigation and Drainage Paper 24.
657 Drerup, P., Brueck, H., Scherer, H.W., 2017. Evapotranspiration of winter wheat estimated
658 with the FAO 56 approach and NDVI measurements in a temperate humid climate of
659 NW Europe. Agricultural Water Management 192, 180–188.
660 doi:10.1016/j.agwat.2017.07.010
661 Er-Raki, S., Chehbouni, A., Boulet, G., Williams, D.G.G., 2010. Using the dual approach of
662 FAO-56 for partitioning ET into soil and plant components for olive orchards in a semi-
663 arid region. Agricultural Water Management 97, 1769–1778.
664 doi:10.1016/J.AGWAT.2010.06.009
665 Er-raki, S., Chehbouni, A., Duchemin, B., 2010. Combining Satellite Remote Sensing Data
666 with the FAO-56 Dual Approach for Water Use Mapping In Irrigated Wheat Fields of a
667 Semi-Arid Region 375–387. doi:10.3390/rs2010375
668 Er-Raki, S., Chehbouni, A., Guemouria, N., Duchemin, B., Ezzahar, J., Hadria, R., 2007.
669 Combining FAO-56 model and ground-based remote sensing to estimate water
670 consumptions of wheat crops in a semi-arid region. Agricultural Water Management 87,
671 41–54. doi:10.1016/J.AGWAT.2006.02.004
672 Er-raki, S., Chehbouni, A., Hoedjes, J., Ezzahar, J., Duchemin, B., Jacob, F., 2008.
673 Improvement of FAO-56 method for olive orchards through sequential assimilation of
674 thermal infrared-based estimates of ET. Agricultural Water Management 95, 309–321.
675 doi:10.1016/j.agwat.2007.10.013
676 Er-raki, S., Rodriguez, J.C., Garatuza-payan, J., Watts, C.J., Chehbouni, A., 2013.
677 Determination of crop evapotranspiration of table grapes in a semi-arid region of
678 Northwest Mexico using multi-spectral vegetation index. Agricultural Water
679 Management 122, 12–19. doi:10.1016/j.agwat.2013.02.007
680 Hanks, R.J., Hill, R.W., 1980. Modeling crop response to irrigation in relation to soils,
681 climate and salinity. International Irrigation Infor- mation Center, 6.
682 Harrold, L.L., Peters, D.B., Dreibelbis, F.R., McGuinness, J.L., 1959. Transpiration
683 Evaluation of Corn Grown on a Plastic-Covered Lysimeter 1. Soil Science Society of
684 America. doi:10.2136/sssaj1959.03615995002300020027x
685 Jacquemin, B., Noilhan, J., 1990. Sensitivity study and validation of a land surface
686 parameterization using the HAPEX-MOBILHY data set. Boundary-Layer Meteorology
687 52, 93–134. doi:10.1007/BF00123180
688 Jin, X., Yang, G., Xue, X., Xu, X., Li, Z., Feng, H., 2017. Validation of two Huanjing-1A/B
689 satellite-based FAO-56 models for estimating winter wheat crop evapotranspiration
690 during mid-season. Agricultural Water Management 189, 27–38.
691 doi:10.1016/J.AGWAT.2017.04.017
692 Khabba, S., Jarlan, L., Er-Raki, S., Page, M. Le, Ezzahar, J., Boulet, G., Simonneaux, V.,
693 Kharrou, M.H., Hanich, L., Chehbouni, G., 2013. The SudMed Program and the Joint
694 International Laboratory TREMA: A Decade of Water Transfer Study in the Soil-Plant-
695 Atmosphere System over Irrigated Crops in Semi-Arid Area. Procedia Environmental
696 Sciences 19, 524–33.
697 Komatsu, T.S., 2003. Toward a robust phenomenological expression of evaporation
698 efficiency for unsaturated soil surfaces. Journal of Applied Meteorology 42, 1330–1334.

699 doi:10.1175/1520-0450(2003)042<1330:TARPEO>2.0.CO;2
700 Lee, T.J., Pielke, R.A., 1992. Estimating the soil surface specific humidity. Journal of Applied
701 Meteorology 31. doi:10.1175/1520-0450(1992)031<0480:ETSSSH>2.0.CO;2
702 Lehmann, P., Merlin, O., Gentine, P., Or, D., 2018. Soil Texture Effects on Surface
703 Resistance to Bare-Soil Evaporation. Geophysical Research Letters 45, 10,398-10,405.
704 doi:10.1029/2018GL078803
705 Leuning, R., Condon, A.G., Dunin, F.X., Zegelin, S., Denmead, O.T., 1994. Rainfall
706 interception and evaporation from soil below a wheat canopy. Agricultural and Forest
707 Meteorology 67, 221–238. doi:10.1016/0168-1923(94)90004-3
708 Luo, C., Wang, Z., Sauer, T.J., Helmers, M.J., Horton, R., 2018. Portable canopy chamber
709 measurements of evapotranspiration in corn, soybean, and reconstructed prairie.
710 Agricultural Water Management 198, 1–9. doi:10.1016/j.agwat.2017.11.024
711 Manabe, S., 1969. Climate and the Ocean Circulation I. The Atmospheric Circulation and the
712 Hydrology of the Earth's Surface. Monthly Weather Review. doi:10.1175/1520-
713 0493(1969)097<0739:CATOC>2.3.CO;2
714 Merlin, O., Al Bitar, A., Rivalland, V., Béziat, P., Ceschia, E., Dedieu, G., 2011. An
715 analytical model of evaporation efficiency for unsaturated soil surfaces with an arbitrary
716 thickness. Journal of Applied Meteorology and Climatology 50, 457–471.
717 doi:10.1175/2010JAMC2418.1
718 Merlin, O., Olivera-guerra, L., Aït Hssaine, B., Amazirh, A., Ra, Z., Ezzahar, J., Gentine, P.,
719 Khabba, S., Gascoin, S., Er-raki, S., 2018. A phenomenological model of soil
720 evaporative e ffi ciency using surface soil moisture and temperature data. Agricultural
721 and Forest Meteorology 257, 501–515. doi:10.1016/j.agrformet.2018.04.010
722 Merlin, O., Stefan, V.G.V.G.G., Amazirh, A., Chanzy, A., Ceschia, E., Er-Raki, S., Gentine,
723 P., Tallec, T., Ezzahar, J., Bircher, S., Beringer, J., Khabba, S., Gentine, P., Er-Raki, S.,
724 Bircher, S., Khabba, S., 2016. Modeling soil evaporation efficiency in a range of soil and
725 atmospheric conditions using ameta-analysis approach. Water Resources Research 52,
726 3663–3684. doi:10.1002/2015WR018233.Received
727 Michel, D., Jiménez, C., Miralles, D.G., Jung, M., Hirschi, M., Ershadi, A., Martens, B.,
728 Mccabe, M.F., Fisher, J.B., Mu, Q., Seneviratne, S.I., Wood, E.F., Fernández-Prieto, D.,
729 2016. The WACMOS-ET project - Part 1: Tower-scale evaluation of four remote-
730 sensing-based evapotranspiration algorithms. Hydrology and Earth System Sciences 20.
731 doi:10.5194/hess-20-803-2016
732 Mutziger, A.J., Burt, C.M., Howes, D.J., Allen, R.G., 2005. Comparison of measured and
733 FAO-56 modeled evaporation from bare soil. Journal of Irrigation and Drainage
734 Engineering 131, 59–72. doi:10.1061/(ASCE)0733-9437(2005)131:1(59)
735 Noilhan, J., Mahfouf, J.-F., Change, G., Change, P., 1996. The ISBA land surface
736 parameterisation scheme. Global and Planetary Change 13, 145–159. doi:10.1016/0921-
737 8181(95)00043-7
738 Noilhan, J., Planton, S., 1989. A Simple Parameterization of Land Surface Processes for
739 Meteorological Models. Monthly Weather Review 117, 536–549. doi:10.1175/1520-
740 0493(1989)117<0536:ASPOLS>2.0.CO;2
741 Ojha, N., Merlin, O., Molero, B., Suere, C., Olivera-Guerra, L., Ait Hssaine, B., Amazirh, A.,
742 Al Bitar, A., Escorihuela, M., Er-Raki, S., 2019. Stepwise Disaggregation of SMAP Soil
743 Moisture at 100 m Resolution Using Landsat-7/8 Data and a Varying Intermediate
744 Resolution. Remote Sensing 11, 1863. doi:10.3390/rs11161863
745 Olivera-Guerra, L., Merlin, O., Er-Raki, S., 2020. Irrigation retrieval from Landsat
746 optical/thermal data integrated into a crop water balance model: A case study over winter
747 wheat fields in a semi-arid region. Remote Sensing of Environment 239, 111627.
748 doi:10.1016/j.rse.2019.111627

Olivera-Guerra, L., Merlin, O., Er-Raki, S., Khabba, S., Escorihuela, M.J., 2018. Estimating the water budget components of irrigated crops: Combining the FAO-56 dual crop coefficient with surface temperature and vegetation index data. Agricultural Water Management 208, 120–131. doi:10.1016/j.agwat.2018.06.014

Parlange, M.B., Katul, G.G., H., C.R., Levent, K.M., Nielsen, D.R., Michael, M., 1992. physical basis for time series model of soil water content. Water Resources Research.

Peters, D.B., 1960. Relative Magnitude of Evaporation and Transpiration 1 . Agronomy Journal 52, 536–538. doi:10.2134/agronj1960.00021962005200090015x

Phillips, T.J., Klein, S.A., Ma, H.Y., Tang, Q., Xie, S., Williams, I.N., Santanello, J.A., Cook, D.R., Torn, M.S., 2017. Using ARM Observations to Evaluate Climate Model Simulations of Land-Atmosphere Coupling on the U.S. Southern Great Plains. Journal of Geophysical Research: Atmospheres 122, 11,524-11,548. doi:10.1002/2017JD027141

Porporato, A., Laio, F., Ridolfi, L., Rodriguez-Iturbe, I., 2001. Plants in water-controlled ecosystems: Active role in hydrologic processes and responce to water stress IV. Discussion of real cases. Advances in Water Resources 24, 745–762. doi:10.1016/S0309-1708(01)00007-0

Raes, D., Steduto, P., Hsiao, T.C., Fereres, E., 2009. AquaCropThe FAO Crop Model to Simulate Yield Response to Water: II. Main Algorithms and Software Description. Agronomy Journal 101, 438. doi:10.2134/agronj2008.0140s

Rafi, Z., Merlin, O., Le Dantec, V., Khabba, S., Mordelet, P., Er-Raki, S., Amazirh, A., Olivera-Guerra, L., Ait Hssaine, B., Simonneaux, V., Ezzahar, J., Ferrer, F., 2019a. Partitioning evapotranspiration of a drip-irrigated wheat crop: Inter-comparing eddy covariance-, sap flow-, lysimeter- and FAO-based methods. Agricultural and Forest Meteorology 265, 310–326. doi:10.1016/J.AGRFORMET.2018.11.031

Rafi, Z., Merlin, O., Le Dantec, V., Khabba, S., Mordelet, P., Er-Raki, S., Amazirh, A., Olivera-Guerra, L., Ait Hssaine, B., Simonneaux, V., Ezzahar, J., Ferrer, F., 2019b. Partitioning evapotranspiration of a drip-irrigated wheat crop: Inter-comparing eddy covariance-, sap flow-, lysimeter- and FAO-based methods. Agricultural and Forest Meteorology 265, 310–326. doi:10.1016/J.AGRFORMET.2018.11.031

Rallo, G., González-Altozano, P., Manzano-Juárez, J., Provenzano, G., 2017. Using field measurements and FAO-56 model to assess the eco-physiological response of citrus orchards under regulated deficit irrigation. Agricultural Water Management 180, 136–147. doi:10.1016/J.AGWAT.2016.11.011

Raz-Yaseef, N., Rotenberg, E., Yakir, D., 2010. Effects of spatial variations in soil evaporation caused by tree shading on water flux partitioning in a semi-arid pine forest. Agricultural and Forest Meteorology 150, 454–462. doi:10.1016/j.agrformet.2010.01.010

Ritchie, J.T., 1972. Model [or PredictingE vaporatio[nr oma Row Crop with Incomplete Cover. Water Resources Research 8, 1204–1213.

Ritchie, J.T., Godwin, D.C., Singh, U., 1989. Soil and weather inputs for the IBSNAT crop models. Proc., IBSNAT Symp.: Decision Support System for Agrotechnology Transfer: Part I., IBSNAT, Dept. Agronomy and Soil Science, College of Tropical Ag- riculture and Human Resources, Univ. of Hawaii, Honolulu, 31–45.

Schlesinger, W.H., Jasechko, S., 2014. Transpiration in the global water cycle. Agricultural and Forest Meteorology 189–190, 115–117. doi:10.1016/j.agrformet.2014.01.011

Steduto, P., Hsiao, T.C., Raes, D., Fereres, E., 2009. Aquacrop-the FAO crop model to simulate yield response to water: I. concepts and underlying principles. Agronomy Journal 101, 426–437. doi:10.2134/agronj2008.0139s

Suleiman, A.A., Ritchie, J.T., 2003. Modeling Soil Water Redistribution during Second-Stage Evaporation. Soil Science Society of America Journal 67, 377.

799 doi:10.2136/sssaj2003.0377
800 Suleiman, A.A., Tojo Soler, C.M., Hoogenboom, G., 2007. Evaluation of FAO-56 crop
801 coefficient procedures for deficit irrigation management of cotton in a humid climate.
802 Agricultural Water Management 91, 33–42. doi:10.1016/j.agwat.2007.03.006
803 Torres, E.A., Calera, A., 2010. Bare soil evaporation under high evaporation demand: a
804 proposed modification to the FAO-56 model. Hydrological Sciences Journal 55, 303–
805 315. doi:10.1080/02626661003683249
806 Twine, T.E., Kustas, W.P., Norman, J.M., Cook, D.R., Houser, P.R., Meyers, T.P., Prueger,
807 J.H., Starks, P.J., Wesely, M.L., 2000. Correcting eddy-covariance flux underestimates
808 over a grassland. Agricultural and Forest Meteorology 103, 279–300.
809 doi:10.1016/S0168-1923(00)00123-4
810 Wallace, J.S., 2000. Increasing agricultural water use efficiency to meet future food
811 production. Agriculture, Ecosystems and Environment 82, 105–119. doi:10.1016/S0167-
812 8809(00)00220-6
813 Wetzel, P.J., Chang, J.-T., 1988. Evapotranspiration from nonuniform surfaces: a first
814 approach for short-term numerical weather prediction. Monthly Weather Review 116.
815 doi:10.1175/1520-0493(1988)116<0600:EFNSAF>2.0.CO;2
816 Wright, J.L., 1982. New evapotranspiration crop coefficients. Journal of the Irrigation &
817 Drainage Division - ASCE 108.
818 Zhang, Y., Shen, Y., Sun, H., Gates, J.B., 2011. Evapotranspiration and its partitioning in an
819 irrigated winter wheat field: A combined isotopic and micrometeorologic approach.
820 Journal of Hydrology 408, 203–211. doi:10.1016/j.jhydrol.2011.07.036
821